IMPACT OF IRON CONTAMINATION ON MINORITY CARRIER LIFETIME OF MULTICRYSTALLINE SILICON SOLAR CELLS

A thesis submitted to

the department of Electrical and Electronic Engineering of

Bangladesh University of Engineering and Technology

in partial fulfillment of the requirement

for the degree of

MASTER OF SCIENCE IN ELECTRICAL AND ELECTRONIC ENGINEERING

by

Mohammad Ziaur Rahman

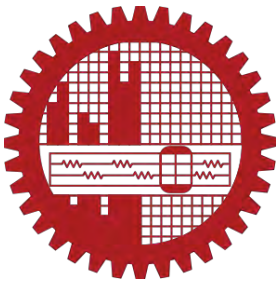

DEPARTMENT OF ELECTRICAL AND ELECTRONIC ENGINEERING

BANGLADESH UNIVERSITY OF ENGINEERING AND TECHNOLOGY

2013

The thesis titled "**IMPACT OF IRON CONTAMINATION ON MINORITY CARRIER LIFETIME OF MULTICRYSTALLINE SILICON SOLAR CELLS**" submitted by Mohammad Ziaur Rahman, Roll No.: 0411062276, Session: April 2011 has been accepted as satisfactory in partial fulfillment of the requirement for the degree of MASTER OF SCIENCE IN ELECTRICAL AND ELECTRONIC ENGINEERING on June 24, 2013.

BOARD OF EXAMINERS

1. …….. **Chairman**
   Dr. Mohammad Jahangir Alam (Supervisor)
   Professor
   Department of Electrical and Electronic Engineering,
   BUET, Dhaka 1000, Bangladesh

2. …… **Member**
   Dr. Pran Kanai Saha (Ex-officio)
   Professor and Head
   Department of Electrical and Electronic Engineering,
   BUET, Dhaka 1000, Bangladesh

3. …… **Member**
   Dr. Quazi Deen Mohd. Khosru
   Professor
   Department of Electrical and Electronic Engineering,
   BUET, Dhaka 1000, Bangladesh

4. …… **Member**
   Dr. Satyendra Nath Biswas (External)
   Professor
   Department of Electrical and Electronic Engineering,
   Ahsanullah University of Science and Technology
   Dhaka 1208, Bangladesh

Declaration

I hereby declare that this thesis or any part of it has not been submitted elsewhere for the award of any degree or diploma.

Signature of the candidate

…….

(Mohammad Ziaur Rahman)

Dedicated

To

Zisan

ACKNOWLEDGEMENT

Me, Myself and all my deeds are devoted to my creator almighty Allah. I am the sinner, but I am always under the shade of the blessing of Allah to accomplish what so ever I did, and his mercy knows no bound. I am grateful to my parents who gave me the first birth and brought me up. I am grateful from the very core of my heart to Mr. Hazrat Ali (Head Master, Digholiakandi Government Primary School, Bashgari, Narsingdi) who come to my life as an angel to protect me from being washed away like debris and gave the second birth. He is the one who put the first brick to add some friction to the very slippery walking way of my life.

My heartiest gratitude is extended toward my supervisor, Prof. Dr. Mohammad Jahangir Alam, for being so gentle and kind to allow me to pursue this thesis under his supervision. His timely supervision helped me to come up with this endeavor in stipulated time.

I would like to thanks Prof. Dr. Satyendra Nath Biswas who smilingly took the burden to proof read the part of the manuscript. Although he is running behind a tight schedule, he never said „no"to any of my request. I am thankful to Prof. Dr. Abdur Rahim Mollah (Head, Department of Electrical and Electronic Engineering, Ahsanullah University of Science and Technology) who encouraged and allowed me to use all the facilities of his department.

My sincere thanks also goes to my friends, relatives, all of the teachers who taught me, all of my students, all of my colleagues and many others who love me, keep me in their pray and give me the reasons to live the everyday life.

ABSTRACT

This thesis presents the qualitative analysis of the variation of effective lifetime of minority carrier in n/p-type Si solar cell due to different recombination mechanisms associated with it. There is a direct relation between the minority carrier lifetime and the solar cell efficiency. The higher lifetime of minority carrier results in increased conversion efficiency of silicon solar cell. As silicon wafers are endowed with different crystal defects and grain boundaries, a reduced minority carrier lifetime is observed for both bulk and surface recombination processes that occur through these defects. A detailed knowledge of the role of recombination processes on carrier lifetime will facilitate the design of high efficiency solar cell. A comparative study has been made to analyze the impact of interstitial iron in minority carrier lifetime of multicrystalline silicon (mc-Si). It is shown that iron plays a negative role and is considered very detrimental for minority carrier recombination lifetime. The analytical results of this study are aligned with the spatially resolved imaging analysis of iron rich mc-Si. A numerical study has been carried out to extract bulk recombination lifetime of minority carrier in Fe contaminated p-type compensated silicon solar cell. It has demonstrated that the compensation will lead to a substantial increase in both intrinsic and Shockley-Read-Hall (SRH) lifetime for minority carrier in p-Si. To understand the role of deliberate phosphorus doping in the minority carrier lifetime of iron contaminated boron-phosphorus-compensated p-type solar grade silicon, another numerical study has been performed. This study confirmed that compensation results a significant increase in bulk lifetime of minority carrier. The gain in carrier lifetime is predicted due to the shift in Fermi energy level, carriers screening and reduction in net equilibrium hole concentration. The bulk lifetime of minority carrier reaches its maximum for phosphorus concentration around 10^{15} cm^{-3} if the boron concentrations remain fixed at 10^{17} cm^{-3}. The utmost importance of this result is the control of compensation level that will facilitate strong improvements in silicon solar cell efficiencies.

LIST OF CONTENTS

LIST OF PUBLICATIONS

Following publications have been produced so far from this thesis:

[1] **Mohammad Ziaur Rahman**, Mohammad Jahangir Alam, "SRH Recombination Strength of Fe in Compensated Solar Grade Silicon", Photonics letters, Poland, 2013 (under review).

[2] **Mohammad Ziaur Rahman**, Mohammad Jahangir Alam, "Enhancement of Minority Carrier Lifetime of Fe Contaminated Boron-Phosphorus Compensated p-Type SoG Silicon", Photonics letters, Poland, **5**(2), 75-77(2013).doi:10.4302/plp.2013.2.14

[3] Mohammad Jahangir Alam, **Mohammad Ziaur Rahman**, "Correlation of Fe-rich Defect Centre and Minority Carrier Lifetime in p-Type Multicrystalline Silicon", Journal of Advanced Materials, 2013 (Accepted for publication).

[4] **Mohammad Ziaur Rahman**, Mohammad Jahangir Alam, "Extraction of Bulk Recombination Lifetime of Minority Carrier in Compensated p-Si Solar Cell", Int. J. of Material Scinence and Electronic Research, 2012 (Accepted for publication).

[5] **Mohammad Ziaur Rahman**, "Modelling Minority Carrier‟s Recombination Lifetime of p-Si Solar Cell" Int. Journal of Renewable Energy Research, Vol. 2 (1), 449 – 454, (2012).

LIST OF FIGURES

LIST OF TABLES

CHAPTER 1

INTRODUCTION

1.1 INTRODUCTION

The initial cost and the low energy conversion efficiency of PV compared to other fuels are the primary barriers preventing it becoming a bigger player in the world energy market. The centre-piece (and at the same time the most costly part) of a photovoltaic module is the solar cell. The semiconductor material, in turn, comprises 65% of the costs involved in fabricating a solar cell. The lion‟s share of wafers (90%) used in the PV industry is made from silicon in either single or multicrystalline form. Silicon owes its dominance to the fact that it is one of the most abundant minerals in the earth crust [1]. It has a band gap of 1.12 eV, which is almost optimal for solar conversion. What gave the silicon technology a major head start was certainly the fact that the PV industry could build up on an existing wealth of research and technology developed by the microelectronics industry. Moreover, efficiencies of 20–25% for single crystalline cells compared to 10–18% for other technologies (apart from multi-junction and concentrator cells) have been reached in the laboratory [2].

At present 90% of solar cells fabricated worldwide are made out of crystalline silicon. An important approach to reduce the costs of these cells is to increase their energy conversion efficiency. As efficiency is strongly related to material quality, the analysis of electrically active defects, which may be introduced during crystal growth or during the solar cell manufacturing process, is of special importance, since these defects in general limits the material quality. A prominent example of such recombination-active defect is metastable defect in industrially used monocrystalline CZ silicon. The carrier lifetime decrease by 90% of its initial value when the defect is activated, which leads directly to a relative efficiency loss of 10% in high efficiency solar cells [3]. An improvement of device performance requires the reduction or avoidance of such recombination active defects which in turn requires their identification in order to identify critical process steps and to provide a reasonable starting – point for process optimization.

In the last few years the market for PV modules has undergone tremendous growth at an annual rate of 34%. The resulting average growth rate since 1983 is then 16.6% pa. A major determinant of increased market growth will be the reduced costs of solar PV [2]. The ability to achieve

continued cost reductions depends largely on the improved cell efficiency. A large proportion of the costs of installed PV systems are area dependent. Therefore, if cell efficiency can be increased without increasing the manufacturing cost, significant reductions in energy cost can be achieved. A high efficiency approach is all that more important to make the best use of the high material cost.

1.2 BACKGROUND AND PRESENT STATE OF THE PROBLEM

The metals that form deep energy levels in silicon belong to transition metals. The 3d transition metals are the main impurities found in silicon during device fabrication [4-6]. There are many ways to introduce impurities into silicon wafers or onto their surfaces by means of solid-liquid, or vapor-phase contamination. Transition metals dissolved in silicon are electrically active and exhibit deep energy levels which act as donor or acceptor states [5]. They may affect the doping concentration in the silicon sample if the impurity concentration is sufficiently high, exceeding the original-charge carrier concentration by a few percent. A severe deterioration of the electrical properties is expected from dissolved impurities with high minority-carrier capture cross sections. A high capture cross section causes a drastic reduction of minority carrier life time in this silicon sample, which still depends on the respective impurity concentration [5,6]. Iron is considered one of the major contaminants in silicon wafer manufacturing processes. The presence of iron in silicon wafers act as recombination centre, particularly for Shockley-Read-Hall (SRH) recombination [7-11]. So a detrimental impact of Fe on carrier lifetime is presumed.

Iron in silicon for solar cells commonly limits the performance of multicrystalline solar cells. In order to reduce its detrimental effect on the recombination lifetime and the cell performance, the quantitative and spatially resolved detection of iron in silicon wafers at different process steps is very important. The qualitative interpretation of lifetime in intentionally Fe-contaminated mc-Si solar cells is studied in this thesis. This thesis is also put an attempt to extract minority carrier lifetime in compensated mc-Si.

1.3 OBJECTIVE OF THE THESIS

The aims of this thesis are:

i. The interpretation of carrier lifetime in multicrystalline silicon which will give an understanding to have a clearer picture of the limiting mechanisms in solar cells made with mc-Si, and points to possible paths for improvement.
ii. Manipulate the role of iron (Fe) in Si solar cells.
iii. Modelling the recombination lifetime of minority carriers in Fe contaminated Si.
iv. Compare the impacts of Fe contamination on minority carrier lifetime for compensated Si solar cells.

1.4 OUTLINE OF THE THESIS

Current solar cell research is based on three pillars representing different aspects and strategies to lower costs and improve cell performance: technology, characterization and simulation. The first field of inquiry encompasses the development of new solar cell concepts that ensure cheaper production (by lowering wafer thickness or cutting down process steps) and new fabrication technologies (e.g. new types of furnaces for the emitter diffusion that allow higher throughput or better emitter quality, implementation of sputtering techniques for the deposition of surface passivation layers). The second research activity seeks to unearth the sources of performance losses, and tries to devise ways of improving energy conversion. The third category engages with a deep physical understanding of the solar cell by modelling it in the best possible way in accordance with the current wealth of knowledge available. The aim of this thesis builds on the second pillar of solar cell research and to be more specific, on mastering recombination losses in silicon solar cells by means of characterization.

Chapter 1 describes the motivation, objectives and aims of the thesis.

Chapter 2 describes the fundamental behavior of 3d transition metals impurities in silicon. The shallow and deep level impurities, their impacts and sources of contamination are highlighted in this chapter. This chapter also describes the properties of iron (Fe) in silicon. The solubility,

diffusivity and electrical activity of Fe in Si are described here. Iron forms complexes with other metal impurities, so redistribution of iron in multicrystalline silicon are important. The quantitative interpretation of iron and the origin of low lifetime of minority carrier hence enumerated here.

Chapter 3 deals with the fundamental concept of generation and recombination mechanisms in multicrystalline silicon (mc-Si). Concept of minority carrier lifetime and different recombination mechanisms associated with mc-Si are analyzed in details. This information presented here serves as the base of the rest of the thesis.

Chapter 4 presents the modelling of minority carrier lifetime in mc-Si. The simulated results of impact of intrinsic and extrinsic recombination on carrier lifetime have shown herewith.

Chapter 5 presents the analytical modelling of minority carrier lifetime of intentionally Fe contaminated mc-Si solar cells. The impact of Fe is explored in depth to find their role in minority carrier lifetime.

Chapter 6 presents the results of carrier lifetime due to Fe contamination on compensated solar grade silicon. A comparison of carrier lifetime of uncompensated electronic grade silicon and compensated solar grade silicon is illustrated here.

Chapter 7 describes the conclusion and suggestions for future works.

CHAPTER 2

PROPERTIES OF IRON IN SILICON

2.1 3d TRANSITION METALS IN SILICON

The metal that forms deep energy levels in silicon belongs to the transition metals. The 3d transition metals are the main impurities found in silicon during device fabrication. The symbol 3d denotes the outer electron configuration of the neutral atom. The presences of transition metals in silicon are considered to be detrimental for the performances of semiconductor devices. For instance, 0.001 ppm titanium reduces the efficiency of silicon based solar cells by 50% [12]. Unfortunately, transition metals are extremely hard to avoid in the semiconductor devices production process. The progressing miniaturization of semiconductor devices therefore requires a detailed understanding of the properties of transition metal related defects.

2.1.1 FUNDAMENTAL BEHAVIOR OF TRANSITION METALS

The concentration and extension of the contaminated volume of 3d transition metals within the silicon wafers depend on the temperature, solubility and diffusivity of the respective impurity metals. The solubility and the diffusivity of the 3d impurity metals are the exponential function of T according to the following Arrhenius equations [5]

$$S = S_0 \exp\left(S_s - \frac{H_s}{kT} \right) \quad (T < T_{eut}), \tag{1.1}$$

$$D = D_0 \exp\left(-\frac{H_M}{kT} \right) \tag{1.2}$$

Where S_s and H_s are the solution entropy and enthalpy, respectively, H_M the migration enthalpy, k the Boltzmann constant, S_0 and D_0 are the temperature independent pre-exponential factors, and T_{eut} is the eutectic temperature. The solubility and diffusivity of common 3d transition metals are shown fig 2.1 and 2.2, respectively.

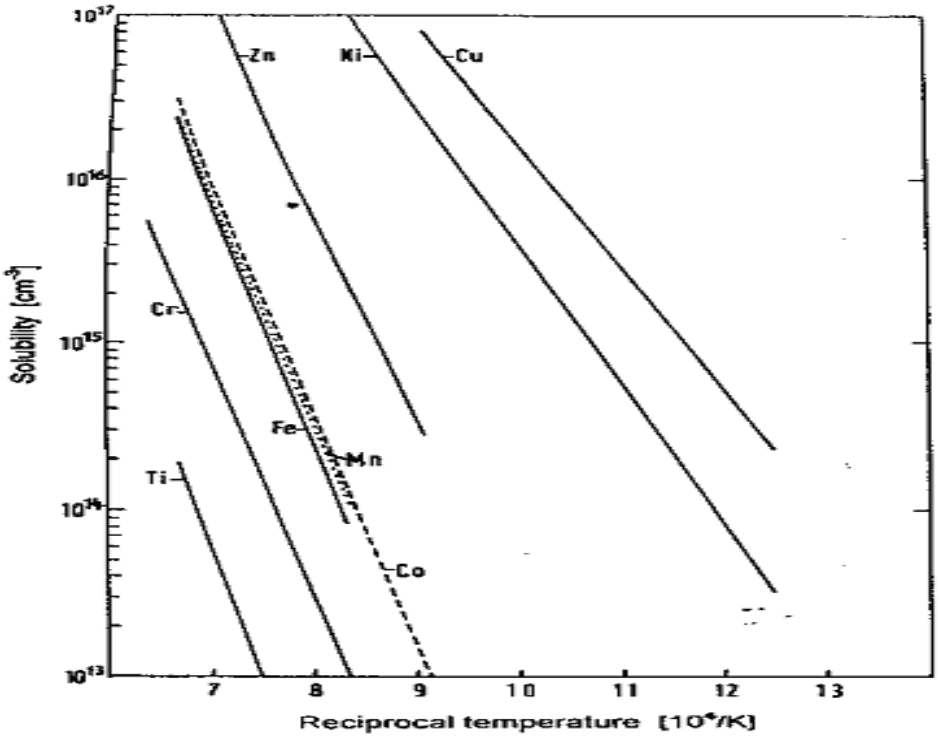

Fig. 2.1 Solubilities of 3d transition metals as a function of inverse temperature [5].

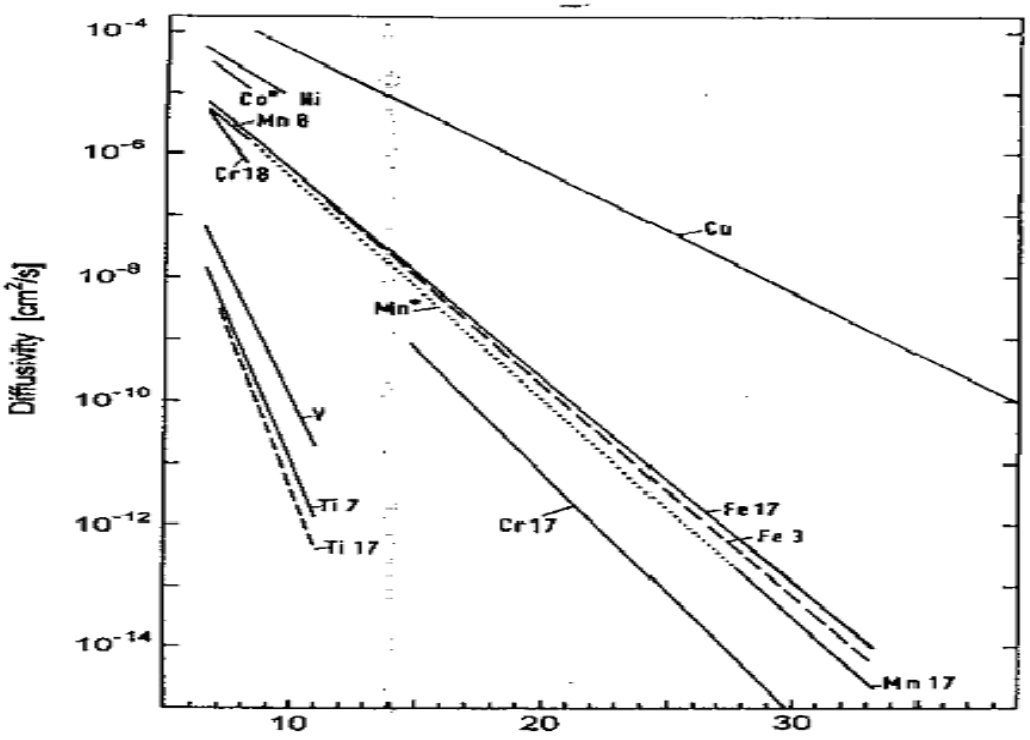

Fig.2.2 Diffusivity of 3d transitional metals as a function of sample inverse temperature [5].

Depending on the temperature treatment (i.e. high temperature diffusion or low temperature cooling), there are three phenomena normally observed for 3d transition metals: precipitation, outdiffusion, and forming electrically active deep energy levels within the band gap of silicon.

The impurity atoms that remain dissolved due to low diffusivity within the volume of the wafer exhibits charge states such as double donors, donors, acceptors, and double acceptors. These metastable impurities tend to form complexes with other impurities in the form of donor-acceptor pairs. Pairs can be formed with both the shallow and deep acceptors of other transition metals and with each other in some particular cases.

2.1.2 SHALLOW AND DEEP LEVEL TRANSITION METALS IN SEMICONDUCTOR

Because the Hamiltonian of a perfect crystalline solid shows the translational symmetry of the lattice, the wave functions describing the electronic states must transform according to one of the irreducible representations of the space group. In the commonly applied one electron band theory of electronic structure this requirement is met by imposing this symmetry on the one-electron state functions resulting in the well known Bloch functions. When applied to semiconductors, band theory results in a band structure showing occupied valence orbitals and unoccupied conduction orbitals grouped in bands and separated by a forbidden energy gap. For semiconductors this energy gap typically is about 1 eV.

States with energy levels in the gap can only appear if the translational symmetry of the perfect lattice is broken, e.g. if the crystal contains imperfections like impurities or lattice vacancies. Such imperfections are always present in real crystals, either as a result of the crystal growth process or introduced deliberately in order to influence the electronic properties of the material. Despite the enormous variation in chemical properties of these imperfections most of them have one feature in common: they introduce energy levels in the gap. Often even more than one charge state produce such gap levels. This amazing property can be explained if one assumes a considerable amount of delocalization of the impurity wave functions into the host region for the absolute values of electron binding energies of the atoms and their variation throughout the periodic system are well outside the energy span of the band gap of any semiconductor. Because of the aforementioned delocalization one cannot separate host and impurity, but has to treat both on the same theoretical footing.

Considering the position of the defect-associated gap levels, two types of impurities can be distinguished [13].

2.1.2.1 SHALLOW LEVEL IMPURITIES

Shallow level impurities are those impurities whose gap levels are positioned very close to one of the band edges: transfer of either an electron from the impurity to the conduction band or a hole from the impurity to the valence band is associated with an energy difference that is much smaller than the band gap width and is typically several meV's. Therefore they contribute significantly to the charge carrier concentration in the host. Donor levels are positioned close to the conduction band, acceptor levels close to the valence band. Shallow level impurities are applied in semiconductors in order to produce semiconductor devices with either n-type (electrons) or p-type (holes) conduction. Junctions between n- and p-type materials have very interesting properties which makes them important in semiconductor device technology.

2.1.2.2 DEEP LEVEL IMPURITIES

Deep level impurities give rise to gap levels that are not close to one of the band edges but are positioned deep in the forbidden gap. Energy differences associated with transfer of electrons from or to these impurities are typically comparable to half the band gap. In most cases gap levels are present for more than one charge state of the impurity, negative as well as positive. Therefore, deep level impurities are very efficient recombination centers for charge carriers, thus reducing the carrier lifetime considerably. In devices, where carrier lifetime must be controlled, small amounts of deep level impurities that are diffused into the crystal can degrade the performance significantly. An in-depth knowledge of the electronic properties of deep level impurities can show the way to techniques for suppression of the unwanted effects and to techniques for efficient application of the desired effects.

2.2 SOURCES OF 3d TRANSITION METALS CONTAMINATION IN SILICON WAFERS

The impurity contamination into silicon wafers or onto their surfaces can be classified into three different mechanisms: the solid-phase, the liquid-phase, and the vapor-phase contamination.

2.2.1 SOLID-PHASE CONTAMINATION

The mechanical contact of the wafer with tweezers (a piece of metal for handling facility) or a contaminated carrier is the main source of solid-phase contamination. Evaporation of metals onto silicon wafer surface is another source of contamination and can introduce various others interfering impurities [14-15]. Sputtering and Ion implantation can also introduce unwanted contamination and are the reasons for different kinds of intrinsic defects which may affect the diffusivity of the metal to be investigated [16-17].

The mechanical contamination may give rise to lattice distortion in the silicon sample surfaces which in turns cause the formation of dislocation and stacking faults in silicon during a subsequent heat treatment [5].

2.2.2 LIQUID-PHASE CONTAMINATION

In the process of device fabrication, silicon wafers may go through different sorts of cleaning processes with liquid solutions. When silicon wafers come in contact with these liquids, transition metals may segregate from the solutions onto the silicon surfaces due to electrochemical and electronegativities nature of the respective metals. Particularly, the metals having eletronegativity higher than that of silicon (≥ 1.8) are preferentially segregate on silicon surfaces [5]. A partial list of transition metals having eletronegativity ≥ 1.8 is shown in the table 2.1.

Table 2.1: Electronegativities of few transition metals (Si = 1.8) [5].

Fe	Co	Mo	Cu	Ag	Pt	Au
1.8	1.8	1.8	1.9	1.9	2.2	2.3

2.2.2 VAPOR-PHASE CONTAMINATION

The oxidation, diffusion in furnace tubes, dry plasma etching, ion implantation, chemical vapor deposition, evaporation and sputtering processes for contact formation are the sources of vapor-phase contamination of silicon wafers with 3d transition metal impurities.

2.3 IRONS IN SILICON

Iron [Fe] is a major contaminant in silicon for solar cells. A minute concentration of iron in silicon is quiet detrimental for the performance of multicrystalline solar cells. Iron is a moderately-fast diffusing 3d transition metals. It has a position in the middle of the sequence of 3d transition metals. During quenching or moderately-fast cooling, iron forms electrically active defects and it precipitates on the sample following the high temperature or annealing treatment at slow cooling [5]. There are both substitutional and interstitial iron may presents in silicon. The substitutional iron is not stable in silicon. Electrically active interstitial iron exhibits only one donor level in the lower half of the band gap. In p-type wafer, interstitially dissolved iron forms donor-acceptor pairs with boron, aluminium, gallium and indium. The pairs shows donor levels with activation energy between 0.1 – 0.2 eV from the valence band edge. Iron forms two energy states, a donor and an acceptor state, when pairs with gold [5, 18].

2.3.1 SOLUBILITY AND DIFFUSIVITY OF Fe IN Si

The solubility of an impurity is defined as the maximum impurity concentration which can be dissolved in thermal equilibrium in a sample at a given temperature. It depends on the surface conditions of the sample. On the other hand, diffusivity is the bulk property. Low diffusivities of the impurity metals are responsible for forming any electrically active, metastable defects in silicon. The solubility and the diffusivity of the iron in silicon can be calculated from the following two Arrhenius equations

$$S_{Fe} = 5\times10^{22}\exp\left(8.2-\frac{2.94}{kT}\right)[cm^{-3}] \quad (900^0C < T < 1200^0C) \qquad [2.1]$$

$$D_{Fe} = 1.3\times10^{-3}\exp\left(\frac{-0.68}{kT}\right)[cm^2/s] \quad (30^0C < T < 1200^0C) \qquad [2.2]$$

2.3.2 ELECTRICAL ACTIVITY OF Fe IN Si

Substitutional iron in silicon is unstable. Interstitial iron forms a neutral state and a positively charged donor state which is situated in the lower half of the band gap with activation energy [5] of

$$E_T = E_V + 0.38\,eV \ . \qquad [2.3]$$

The activation energies of iron with various shallow and deep acceptors are listed in table 2.2 and 2.3, respectively.

Table 2.2: Activation energies (Act. En.) of Fe-shallow acceptor pairs

Pair	Ac. En. [eV]	donor/acceptor	Ref.
FeB	Ev + 0.10	donor	[19]
	Ec - 0.23	acceptor	[20]
FeAl	Ev + 0.19	donor	[19]
	Ev + 0.13	donor	[21]
FeGa	Ev + 0.24	donor	[19]
	Ev + 0.14	donor	[20]
FeIn	Ev + 0.27	donor	[20]
	Ev + 0.16	donor	[20]

In p-type silicon interstitial iron acts as a lifetime killer. The majority carrier cross-section in p-type silicon can be determined from the following equation [23]

$$\sigma_h(Fe_i) = 5.6\times10^{-16}\exp\left(\frac{-0.048}{kT}\right) \quad [cm^2] \qquad [2.4]$$

Table 2.3: Activation energies (Act. En.) of Fe-deep acceptor pairs

Pair	Ac. En. [eV]	donor/acceptor	Ref.
FeAu	Ev + 0.43	donor	[22-24]
	Ec - 0.35	acceptor	[22-24]
FeZn	Ec - 0.47	donor	[22-24]

The minority carrier capture cross-section was reported as [25]

$$\sigma_n(Fe_i) = 2.6\times10^{-14} \quad [cm^2] \qquad [2.5]$$

Minority carrier lifetime or diffusion length in p-type silicon has been used to detect and determine the Fe concentrations [26].

2.3.3 COMPLEXES OF Fe WITH OTHER IMPURITIES

Iron is always present in even processed wafer in minor concentration. Being the moderately-fast diffuser, iron exhibits mobility that is not too low at rapid thermal (RT) annealing. Iron, hence, has a tendency to form complexes and pairs with other impurities to acquire a more stable state in the silicon host lattice. Donor-acceptor pairs are formed between the positively-charged donor state of the interstitial iron and the negatively-charged acceptor state of the doping element which is usually boron in p-type silicon. In a iron contaminated p-type silicon, the Fermi level lies between the energy level of the iron donor (E_V + 0.38 eV) and the energy level of the boron acceptor (E_V + 0.044 eV) for a doping concentration of over 10^{14} cm^{-3} [5]. Therefore, the iron donor state is positively charged and the boron acceptor state is negatively charged.

At RT, substitutional boron is immobile. The interstitial iron then diffuse through the silicon lattice to approach a boron atom, and iron-boron pair is formed as a result of columbic attraction. The reaction is diffusion limited and intensely dependent on the boron concentration in silicon. Usually iron concentration is orders of magnitude lower than the boron concentration, and iron,

therefore, doesn‟t noticeably influence the reaction time. The reaction time depends on the iron and boron concentration and the resistivity of the sample. As a rule of thumb, lower the resistivity of the given sample, faster the pairing. The pairing reaction can be observed from the deep level transient spectroscopy (DLTS).

$$[Fe^+]+[B^-]\leftrightarrow[Fe^+B^-] \qquad [2.6]$$

The equilibrium is shifted towards the iron-boron (FeB) pairs at low temperature (0^oC) and towards the dissociated pairs at about 200^oC. AT high temperature, iron starts to precipitate and interstitial iron concentration gets reduced with time. The pairing and dissociation can also be happened when the sample is subjected to the intense light. When the sample is being illuminated, electron-hole-pairs (EHP) are generated which shift the quasi-Fermi level toward the mid gap. As a result, electrostatic attraction between iron and boron reduced, and iron don‟t form pair with boron [27]. Minority carrier injection thorough a pn-junction is another way to iron-boron pairs dissociation and shows a linear dependence on the injection level. The electrostatic binding energy for FeB pair at low injection is about 0.45 eV [28]. FeB pairs formation increase the resistivity and the minority carrier lifetime of a sample at low injection [26].

FeB pair forms a donor state in the lower half of the silicon band gap (E_V + 0.1 eV) [27] and an acceptor state in the upper half of the band gap (E_C – 0.23 eV) [29].

2.4 REDISTRIBUTION OF Fe IN MULTICRYSTALLINE SILIOCN

Iron is a major contaminant in silicon for solar cells which commonly limits the performance of multicrystalline solar cells. In order to reduce its detrimental effect on the recombination lifetime and the cell performance the quantitative and spatially resolved detection of iron in silicon wafers at different process steps is very valuable.

A model of Fe distribution in mc silicon has been implemented in Sentaurus Process by Jonas Schön et al. [30] taking segregation to high dislocated regions and precipitation at extended defects into account. Simulations of the Fe diffusion and accumulation at extended defects after solidification of mc silicon were compared to experimental results. The interstitial and total Fe concentrations over block height correspond well with experimental results.

The simulation for the ingot contaminated with $1 \cdot 10^{18}$ cm^{-3} Fe results in a noticeable proportion of precipitated Fe in low dislocated areas also for medium heights ($2\text{-}5 \cdot 10^{12}$ cm^{-3}). However, the simulation of the Fe_i distribution (Fig. 2.3a) exhibits that most of the Fe in low dislocated grains is in the interstitial state. In contrast the Fe_i concentrations in areas of high dislocation density do not significantly depend on the contamination level. This leads to a remarkable higher Fe_i concentration in lowly dislocated grains than in the adjacent grain boundaries with high dislocation density. The Fe_i image (Fig. 2.3b) of a wafer (at 34% ingot height) shows a high contrast between grains and grain boundaries, too.

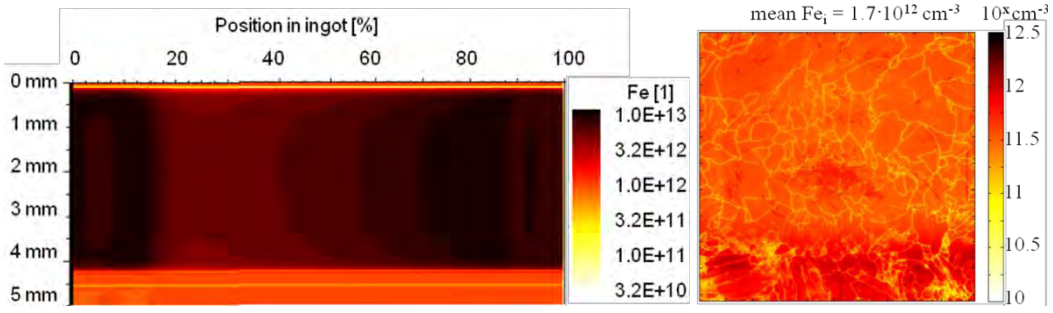

(a) (b)

Fig. 2.3: Simulated (a) and measured Fe_i (b) concentration after cooling down for an ingot intentionally contaminated with $1 \cdot 10^{18}$ cm^{-3} Fe [30].

2.5 QUANTITATIVE DETERMINATION OF Fe CONCENTRATION

A very specific and simple technique to detect the interstitial iron concentration quantitatively consists of the interpretation of two lifetime measurements on the same sample under different conditions: One measurement is performed on an annealed sample where instead of interstitial iron only iron-boron pairs are present and a second measurement where the iron-boron pairs are completely decomposed as shown in fig.2.4. Since the defect properties such as energy level and capture cross section differ from one to the other state, differences in the measured recombination lifetime occur.

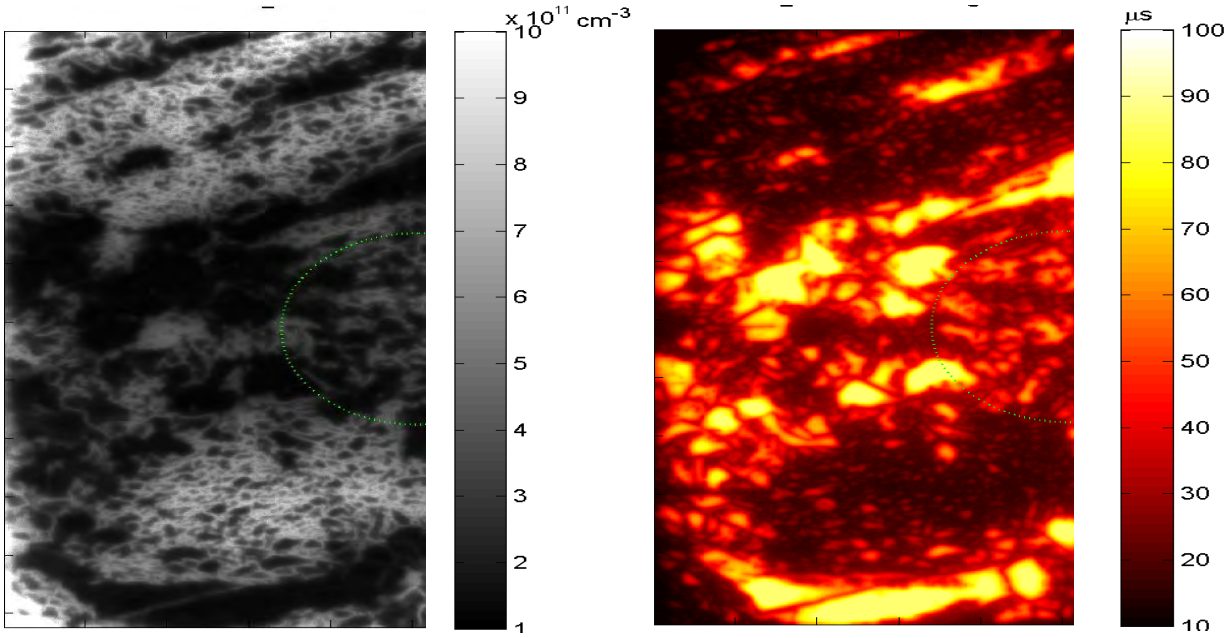

Fig.2.4: Quantitative imaging of interstitial iron (left) based on lifetime measurements before and after light soaking and recombination lifetime image on same sample of multicrystalline silicon (right) [31].

An algorithm has been deduced by Macdonald et al. [31] for the calculation of the iron concentration from two lifetime measurements at two different injection levels for p-type crystalline silicon. The algorithm results in the following equations

$$[Fe_i] = \frac{1}{\chi^{Fe_i} - \chi^{FeB}} \left| \left(\frac{1}{\tau_1} + \frac{1}{\tau_{Auger,0}} \right) - \left(\frac{1}{\tau_0} + \frac{1}{\tau_{Auger,1}} \right) \right| \quad with \qquad [2.7]$$

$$\chi^{Fe_i} = \frac{v_{th}(N_A + \Delta n_1)}{\frac{1}{\sigma_n^{Fe_i}}\left(N_A + p_1^{Fe_i} + \Delta n_1\right) + \frac{\Delta n_1}{\sigma_p^{Fe_i}}} \qquad [2.8]$$

$$\chi^{FeB} = \frac{v_{th}(N_A + \Delta n_0)}{\frac{1}{\sigma_n^{FeB}}\left(N_A + \Delta n_0\right) + \frac{1}{\sigma_p^{FeB}}\left(n_1^{FeB} + \Delta n_0\right)} \qquad [2.9]$$

where N_A is the acceptor concentration, V_{th} is the thermal velocity, $\tau_{0/1}, \tau_{Auger0/1}, \Delta n_{0/1}$ are the carrier lifetime, auger lifetime and excess carrier concentration at FeB and Fe_i, respectively.

$\sigma_{n/p}^{Fe_i/FeB}$ the corresponding carrier capture cross section, $p_1^{Fe_i}$ the hole concentration of SRH recombination at $Fe_{i,}$ n_1^{FeB} electron concentration of SRH recombination at FeB.

2.6 ORIGIN OF LOW CARRIER LIFETIME IN mc-Si

Multicrystalline silicon produced by directional solidification are endowed with different sorts of defects, and showed varying carrier lifetime in various region of the silicon wafer. Carrier lifetime is dominated by oxygen-related defects in the bottom and by the high concentration of segregated transition metals at the top of the ingot [32-33]. At the edge zones of the ingot, carrier lifetime is influenced by oxygen-related defects, point-like defects, and precipitates with high concentration of iron [34-35]. At the edge zone, 2-3 order of magnitude increase in Fe concentration was reported due to inward diffusion of iron from the crucible and crucible material [32]. The common opinion is that the contamination by the impurities from the crucible walls is responsible for the reduced lifetime.

Fig. 2.5 shows the variation of minority carrier lifetime as a function of the distance to the edge of mc-Si. At the vicinity of the edge, carrier lifetime less than 1 μs has observed, while it starts increasing at 15-17 mm from the edge. This is due to the high volume presence of dislocations, grain boundaries, twins, drying stains and scratches in the edge zone region compared to in the bulk. The size, orientation and the type of grain and grain boundaries have significant impact on the carrier lifetime.

The grains are normally nucleated along the sidewall of an ingot which results in random angle grain boundaries (RAGB). The RAGB decreases with increase in the distance from the edge. The RAGB is the favorable conditions for precipitation of iron. Dissolved iron, iron complexes and precipitates introduce deep levels in the silicon band gap, and are the known reason for enhanced recombination rate [32, 36].

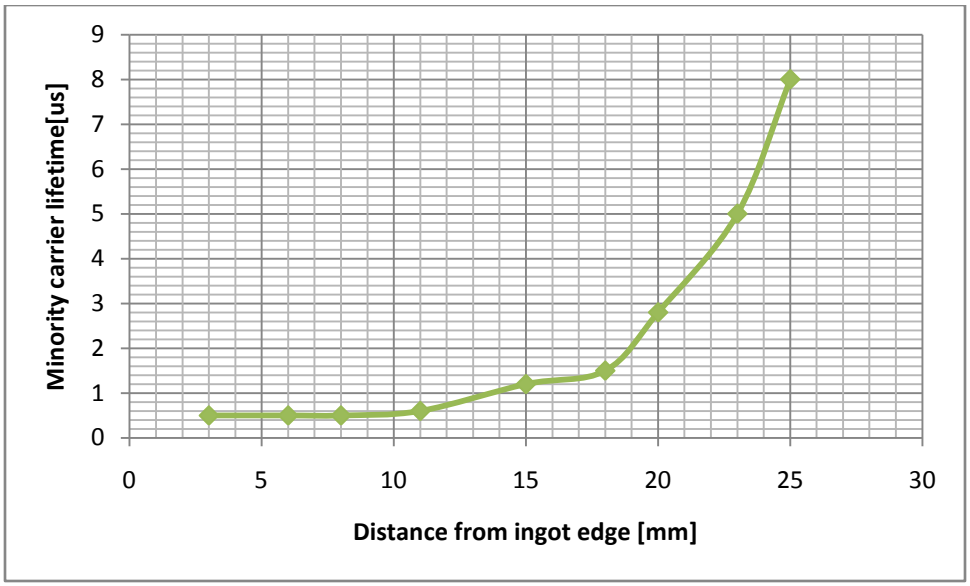

Fig. 2.5: Variation of minority carrier lifetime with distance to the edge of mc-Si ingot.

CHAPTER 3

GENERATION AND RECOMBINATION IN MC-Si SOLAR CELLS

3.1 INTRODUCTION

Solar cell is a photonic device which converts sun light into direct current when appropriate photons are absorbed into the solar cell material. Upon incident a sun ray of defined wavelength on solar cell surface, carriers (electron or hole) generate, and contribute to the generation of photocurrent. So an understanding of photon absorption, carrier transport phenomena, generation and recombination of carriers are very important.

3.1.1 ABSORPTION OF LIGHT IN INDIRECT GAP SEMICONDUCTOR

Light absorption in a material depends on the wavelength of light and the properties of the material. When a monochromatic ray incident on the absorber material surface, parts of it gets reflected and the rest become attenuated while passing through the material. For an infinite thickness of absorber layer, light decay follows the Beer-Lambert law

$$I(z,\lambda) = I_0 e^{-\alpha(\lambda)z} \quad with$$
$$\alpha(\lambda) = \frac{4\pi\kappa}{\lambda} \tag{3.1}$$

where I_0 is the light intensity at the material surface, α is the absorption co-efficient, κ is the extinction coefficient of the material.

Fig. 3.1 shows the dependence of absorption coefficient, α of a crystalline silicon slab on photon energy at T = 300^0K. When a photon is absorbed, electrons in valance band get excited and transported to the conduction band leaving behind a hole in valance band. For silicon, photon energy must be greater than the band gap energy of silicon to excite the valance band electrons to conduction band and should be satisfied the following condition [13]

$$E_{photon} = \frac{1.24}{\lambda[\mu m]} > E_C - E_V = E_g \tag{3.2}$$

The absorption process in an indirect band-gap semiconductor like silicon involves a third particle, the phonon, which is characterized by low energy and high momentum. Therefore the probability of light absorption in these semiconductors is significantly lower than that of direct band-gap materials.

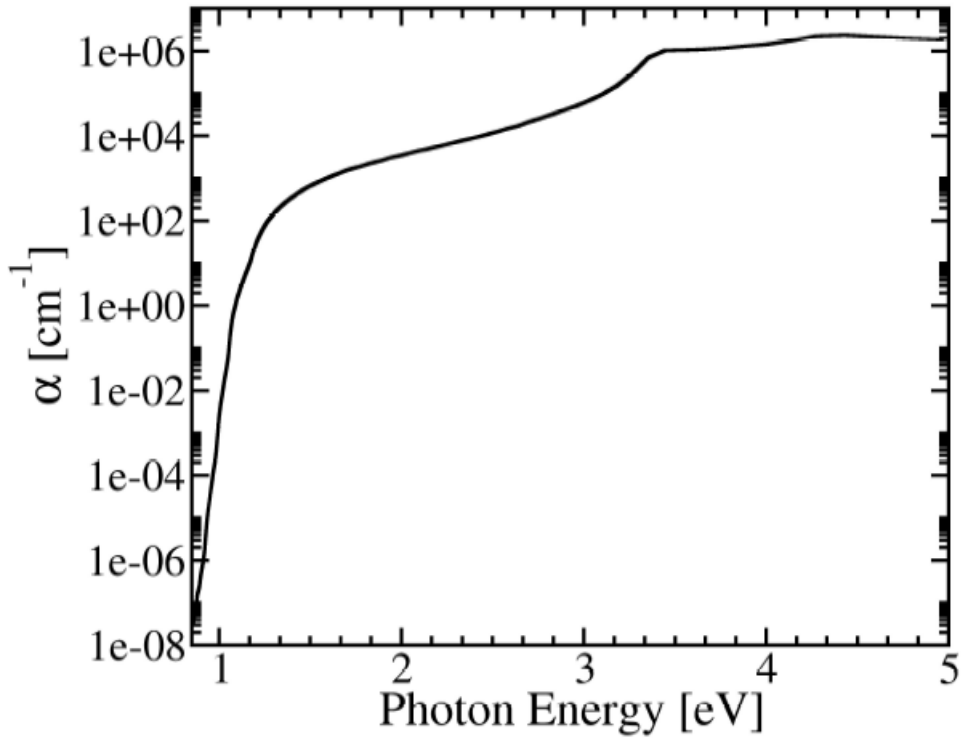

Fig. 3.1: dependence of absorption coefficient, α of a crystalline silicon slab on photon energy at T = 300^0K [13].

3.2 PHOTOGENERATION RATE

Photogeneration means the generation of mobile electrons and holes through the absorption of light in the semiconductor. If it is assume that all the photons are absorbed to generate free carriers then the rate of carrier generation, per unit volume, at a depth z below the surface is given by [37]

$$g(E,z) = b(E,z)\alpha(E,z) \tag{3.3}$$

where *b* is the photon flux at *z*, *E* is the photon energy. We need to consider the reflection of photons at the surface and the attenuation of photons within the bulk of the materials to calculate actual carrier generation rate, g(E,z). Thus

$$g(E,z) = (1-R)\alpha(E)b(E)e^{-\int_0^z \alpha(E,z)dz} \tag{3.4}$$

where *R* is reflectivity of the surface. This is the spectral Photogeneration rate. To find the total generation rate at *z*, it is needed to sum over the photon energies where the photon absorption results in free carrier generation. Thus

$$G_{OPT}(z) = \int g(E,z)dE \tag{3.5}$$

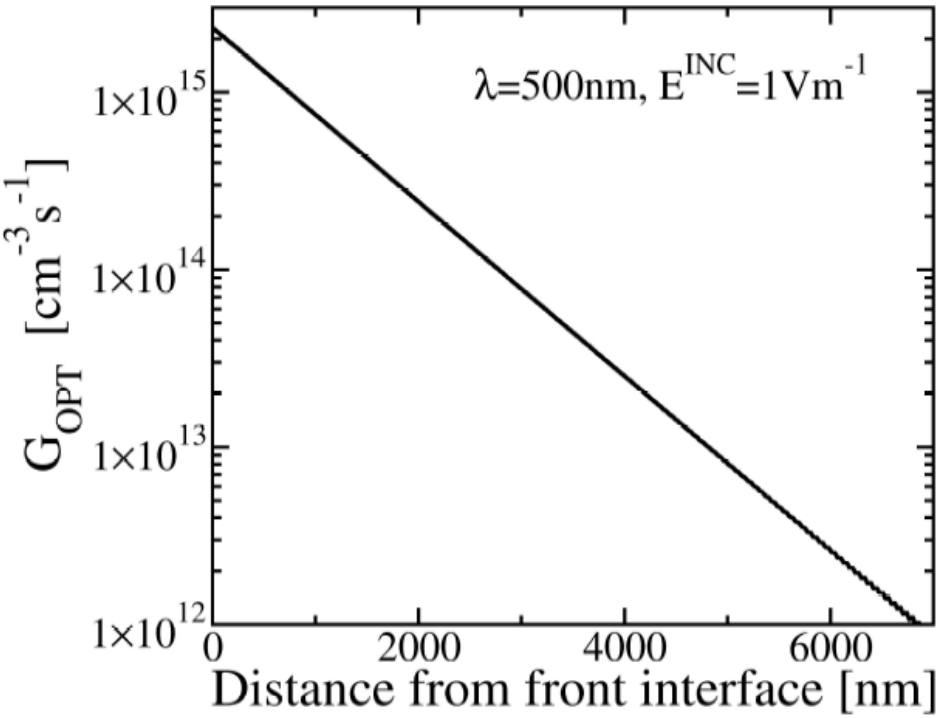

Fig. 3.2: Optical generation rate calculated at λ = 500 nm considering silicon slab has infinite thickness [38].

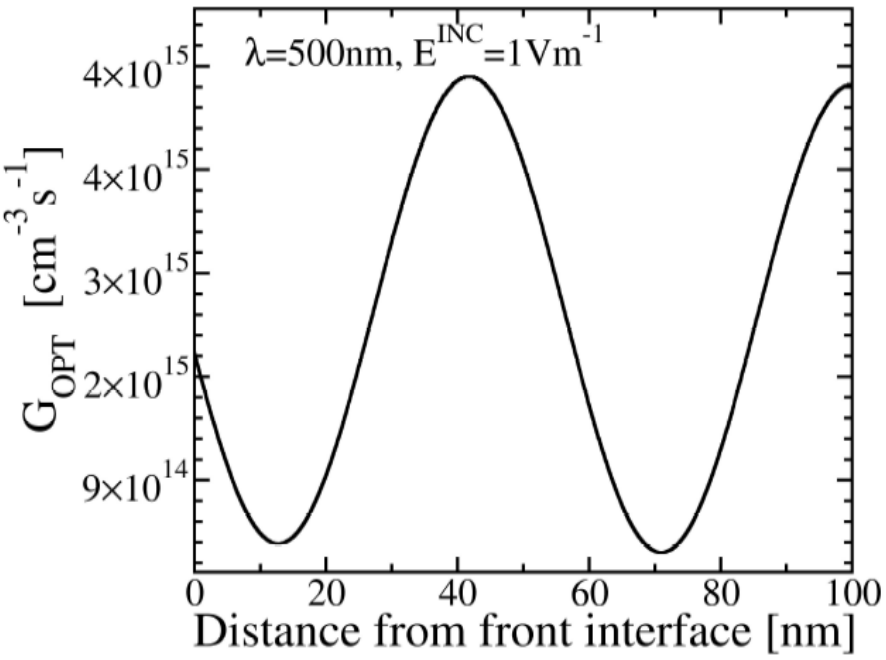

Fig. 3.3: Optical generation rate calculated at λ = 500 nm considering silicon slab has finite thickness [38].

In fig. 3.2, G_{OPT} is calculated for a silicon slab of infinite thickness at λ = 500 nm. If the dimension of the silicon slab is lower the absorption length of photon at a given λ, the Beer-Lambert law is then invalid. In this case, multiple internal reflections of light occur at the front and the back surfaces of the silicon slab, hence a maxima and minima in optical generation rate is generally observed as shown in fig. 3.3.

3.3 FUNDAMENTALS OF GENERATION AND RECOMBINATION

Generation is an electronic excitation event which may define as the promotion of an electron from valence band (VB) to conduction band (CB) to create an electron-hole-pair (EHP), or from VB into a localized state in the band gap to create only a hole, or from a localized state into the CB which generate only an electron. Generation increases the number of free carriers available to carry charge. The energy required for the excitation comes through the thermal vibration of lattice (phonons), or through the absorption of photon, or from the kinetic energy of another

carrier. Generation by absorption of photon is the most important form of generation in solar cell.

Recombination is an electronic excitation event which is the loss of an electron or hole through the decay of an electron to a lower energy state. This may be from band to band to destroy an EHP, or it may be from CB to the trap state or from trap state to VB, removing only an electron or hole, respectively. The energy released in recombination processes can be given as a photon (radiative recombination), as heat through phonon emission (non-radiative recombination) or as kinetic energy to another free carrier (Auger recombination).

Following the net recombination, U_n and net generation, G_n for a given semiconductor material, the rate of change of electron density per unit volume is given by [13]

$$\frac{\partial n}{\partial t} = \frac{1}{q}\frac{\partial}{\partial x} J_n + G_n - U_n \tag{3.6}$$

here J_n is the electron current density.

3.4 CONCEPT OF RECOMBINATION LIFETIME

For every generation process there is an equivalent recombination process. At T = 0^0K, if there is no external bias, electrons occupy all the energy state up to Fermi level and there is a no transition of electrons from VB to CB, hence no recombination or generation process results in. At T > 0^0K, electron gain energy due to lattice thermal vibration and promoted to the higher energy level which may define as thermal generation. Electrons in the excited states, at the same time, can relax down to vacant lower energy state and give up the vibrational energy to the lattice. The loss of an electron in this process is called thermal recombination. At thermal equilibrium, thermal generation G_0 is counter balanced by a recombination R_0 (i.e. $G_0 = R_0$) and the density of electron-hole product remain constant ($n_0 p_0 = n_i^2$).

When the system is perturbed from thermal equilibrium, i.e. for a constant optical excitation, the system passes through a new generation and recombination rate which results in a non-

equilibrium electron, n and hole, p densities with $np > n_i^2$. As the thermal equilibrium cannot be reached instantaneously after switching of the external generation source, there are excess carrier densities $\Delta n = n - n_0$ and $\Delta p = p - p_0$ for electron and hole, respectively. The excess carriers decay successively to reach thermal equilibrium with net recombination rate $U = R - R_0$. The time dependent decay of excess carrier density, for example Δn, follows

$$\frac{\partial}{\partial t}(\Delta n) = -U \ . \tag{3.7}$$

The time constant, τ of this exponential decay is referred to as the *recombination lifetime* or simply, *carrier lifetime*, and is defined as [3]

$$\tau = \frac{\Delta n}{U} \ . \tag{3.8}$$

The carrier lifetime in general strongly depends on the injection density of excess carrier Δn and on the doping concentration of electron and hole.

3.5 RECOMBINATION MECHANISMS

Carrier transport in semiconductor is greatly influenced by different recombination mechanism. Thus, having a very clear understanding about recombination phenomena are utter importance. The recombination mechanisms are broadly categorized as *intrinsic recombination* mechanism and *extrinsic recombination* mechanism. The recombination mechanisms are depicted in fig. 3.4.

When carriers recombine from band to band is termed as intrinsic recombination. Intrinsic recombination is of two types: *radiative recombination* and *Auger recombination*. It is independent of crystal growth process and is always present and unavoidable.

If the decay of an electron-hole-pair via a defect centre with an intermediate energy level is known to as extrinsic recombination mechanism. The intermediate states are due to impurities in

the crystal or defects in the crystal structure. There are two types of extrinsic recombination: bulk *Shockley-Read-Hall (SRH) recombination* and *surface recombination*.

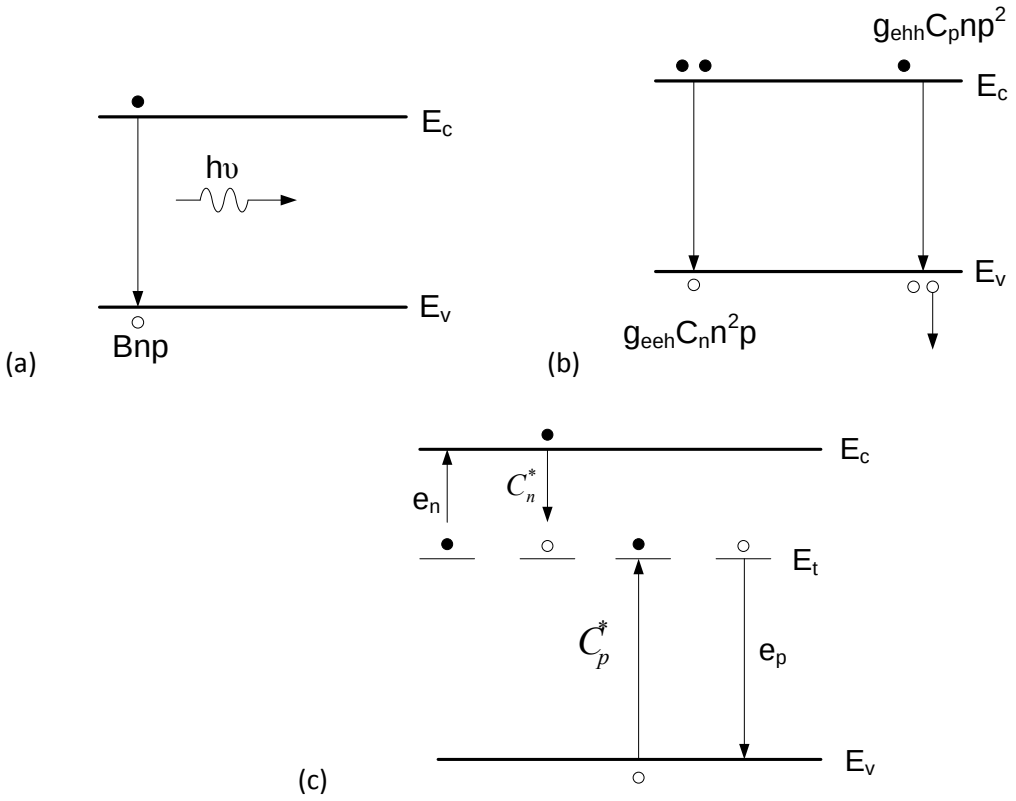

Fig. 3.4: Illustration of different recombination mechanisms.

3.5.1 RADIATIVE RECOMBINATION

Radiative recombination is the reverse process of optical generation. It is a band to band recombination process where a direct annihilation of an EHP occurs as shown in fig. 3.4(a). When an electron from CB comes down to VB to recombine with a hole, it releases the absorbed photon energy which is approximately equal to the semiconductor material band gap. This process depends jointly on electrons and holes concentration. The net radiative recombination rate is given by

$$U_{rad} = B\left(np - n_i^2\right) \tag{3.9}$$

where B is the constant, and represents the quantum-mechanical probability of radiative transition. It strongly depends on the band structure of the semiconductor.

For non-equilibrium concentrations of $n = n_0 + \Delta n$ and $p = p_0 + \Delta p$, and assuming charge neutrality ($\Delta n = \Delta p$), U_{rad} takes the following simplified form

$$U_{rad} = B(n_0 + p_0)\Delta n + B\Delta n^2 \tag{3.10}$$

The radiative recombination lifetime is then become [3]

$$\tau_{rad} = \frac{1}{B(n_0 + p_0)\Delta n + B\Delta n} \tag{3.11}$$

For low level injection ($\Delta n << n_0 + p_0$)

$$\tau_{rad,lli} = \frac{1}{BN_{dop}} \tag{3.12}$$

And for high level injection ($\Delta n >> n_0 + p_0$)

$$\tau_{rad,hli} = \frac{1}{B\Delta n} \tag{3.13}$$

For p-type material

$$\tau_{rad} = \frac{1}{B(N_A + \Delta n)} \tag{3.14}$$

Radiative recombination is the dominant recombination process in direct band gap semiconductor. It has negligible impact in indirect semiconductor compared to other recombination processes.

3.5.2 AUGER RECOMBINATION

Auger recombination is viewed as a three-particle interaction where a conduction band electron and a valence band hole recombine, with the excess energy being transferred to a third free electron or hole, as depicted in fig. 3.4(b) . The charge carriers involved are assumed to be non-interacting quasi-free particles. For band-to-band Auger recombination, an electron and two holes (ehh) or a hole and two electrons are involved (eeh). The *eeh* process denotes when the excess energy is transferred to another electron, with the recombination rate given by $U_{eeh}=C_n n^2 p$. Similarly, the *ehh* process denotes when the excess energy is transferred to another hole, with recombination rate $U_{ehh}=C_p n p^2$, where C_n and C_p are Auger coefficients. The total Auger recombination rate, U_{Auger}, is then given by

$$U_{Auger} = C_n\left(n^2 p - n_0^2 p_0\right) + C_p\left(np^2 - n_0 p_0^2\right) \tag{3.15}$$

from which the common relationships for the Auger lifetime in *n*-type and *p*-type material under low injection ($\tau_{Auger,li}$) and high injection conditions ($\tau_{Auger,hi}$) can be determined. For *n*-type silicon

$$\tau_{Auger,lli} = \frac{1}{C_n N_D^2} \quad and \quad \tau_{Auger,hli} = \frac{1}{\left(C_n + C_p\right)\Delta p^2} \tag{3.16}$$

And for p-type silicon

$$\tau_{Auger,lli} = \frac{1}{C_p N_A^2} \quad and \quad \tau_{Auger,hli} = \frac{1}{\left(C_n + C_p\right)\Delta n^2} \tag{3.17}$$

where $C_a = C_n + C_p$ is the ambipolar Auger coefficient. The most commonly quoted values for the Auger coefficients appear to be those determined by Dziewior and Schmid ($C_n = 2.8\text{x}10^{-31}\text{cm}^6\text{s}^{-1}$ and $C_p = 0.99\text{x}10^{-31}\text{cm}^6\text{s}^{-1}$) for silicon with a doping concentration greater than $5\text{x}10^{18}\text{cm}^{-3}$[39] . The implied value for the ambipolar Auger coefficient is then $C_a = 3.79 \text{ x } 10^{-31}\text{cm}^6\text{s}^{-1}$.

Auger recombination shows a stronger dependence with the injection level than τ_{rad}, and therefore, Auger recombination will become the dominant mode of recombination in silicon for high injection levels, as might occur in concentrator solar cells, or for high dopant densities, as occurs in heavily doped emitter regions.

In reality, Auger recombination is more complicated than the idealised view presented above. The experimental observations consistently pointed towards a mechanism which enhances the Auger recombination at lower densities. The most elegant theoretical explanation for this effect has been presented by Hangleiter and Häcker with their theory of Coulomb-enhanced auger recombination [40]. In traditional theory the charge carriers involved in recombination process are regarded as non-interacting quasi-free particle, whereas they took into account the coulomb interaction between the mobile charge carriers. Due to this coulomb interaction the electron density is locally increased in the vicinity of a hole and locally reduced in the vicinity of an electron. As the Auger recombination rate strongly depends on the carrier concentration, it may significantly increase due to such local inhomogeneities in the carrier density. To account for this effect, the Auger coefficients C_n and C_p in eqn. (2.7) are multiplied by carrier density dependent enhancement factors g_{eeh} and g_{ehh}. Altermatt et al. [41] determined an empirical parameterization for the enhancement factors g_{eeh} and g_{ehh} as following expression

$$g_{eeh}(N_D) = 1 + 44\left\{1 - \tanh\left(\frac{N_D}{5\times10^{16}cm^{-3}}\right)^{0.34}\right\} \tag{3.18}$$

$$g_{ehh}(N_A) = 1 + 44\left\{1 - \tanh\left(\frac{N_A}{5\times10^{16}cm^{-3}}\right)^{0.29}\right\} \tag{3.18}$$

A model for the injection dependence of CE-Auger life time was proposed in [42] and the following expression for Auger coefficients found

$$C_n^* = g_{eeh}C_n\left(\frac{n_0}{n_0+\Delta n}\right) + \frac{C_a}{2}\left(\frac{\Delta n}{n_0+\Delta n}\right) \tag{3.19}$$

$$C_p^* = g_{ehh} C_p \left(\frac{p_0}{p_0 + \Delta p} \right) + \frac{C_a}{2} \left(\frac{\Delta p}{p_0 + \Delta p} \right) \tag{3.20}$$

Using the effective auger coefficients, the injection dependent CE-Auger life time may be calculated as

$$\tau_{CE-AUger} = \frac{n - n_0}{C_n^* \times \left(n^2 p - n_0^2 p_0 \right) + C_p^* \times \left(np^2 - n_0 p_0^2 \right)} \tag{3.21}$$

3.5.3 SHOCKLEY-READ-HALL RECOMBINATION

The presence of defects within a semiconductor crystal due to impurities or crystallographic imperfections such as dislocations, produces discrete energy levels within the band gap. These defect levels, also known as *traps*, greatly facilitate recombination through a two-step process whereby a free electron from the conduction band first relaxes to the defect level and then relaxes to the valence band where it annihilates a hole. Trap state is spatially localised whilst free electron or hole is delocalised, so we can think free carrier as being captured by the trap. The carrier can subsequently be released by thermal activation and injected back to the band from which it comes actually. Trap doesn‟t contribute directly to recombination, but change the free carrier concentrations which have great impact on carrier dynamics. If the trap captures a carrier of the opposite polarity before the first carrier is released, then trap has been emptied again and the two carriers have in effect recombined. Localised states which serve mainly to capture and release only one type of carrier are usually called traps. Those which capture both types of carrier are called recombination centres. Usually recombination centres lie deeper into the band gap than traps.

The dynamics of this recombination process where first analysed by Shockley and Read and Hall [7-8], with the recombination rate, U_{SRH}, for a single defect level given by

$$U_{SRH} = \frac{np - n_i^2}{\tau_{p_0} \left(n + n_1 \right) + \tau_{n_0} \left(p + p_1 \right)} \tag{3.22}$$

Where τ_{n_0} and τ_{p_0} are the fundamental hole and electron lifetimes which are related to the thermal velocity of charge carriers, ν_{th}, the density of recombination defects, N_t, and the capture cross-sections, σ_n and σ_p, for the specific defect:

$$\tau_{p_0} = \frac{1}{\sigma_p \nu_{th} N_t} \qquad and \qquad \tau_{n_0} = \frac{1}{\sigma_n \nu_{th} N_t} \tag{3.23}$$

n_1 and p_1 are statistical factors defined as

$$n_1 \equiv N_C \exp\left(\frac{E_t - E_C}{kT}\right) \qquad and \qquad p_1 \equiv N_V \exp\left(\frac{E_C - E_G - E_t}{kT}\right) \tag{3.24}$$

here N_C and N_V are the effective density of states at the conduction and valence band edges, E_C and E_G are the conduction band and band gap energies and E_t is the energy level of the defect.

For an arbitrary concentration of recombination centres N in a non-degenerate semiconductor with no significant drift or diffusion currents under general illumination condition, following first order differential equations have been developed [6]

$$\frac{d}{dt}\Delta n = \frac{\Delta n}{\tau_n} = g_e - \frac{1}{\tau_{n_0}}\left[\frac{(n_0 + n_1 + \Delta n)(\Delta n - \Delta p)}{N} + \frac{\Delta n n_1}{n_0 + n_1}\right] \tag{3.25}$$

$$\frac{d}{dt}\Delta p = \frac{\Delta p}{\tau_p} = g_e - \frac{1}{\tau_{p_0}}\left[\frac{(p_0 + p_1 + \Delta p)(\Delta p - \Delta n)}{N} + \frac{\Delta p p_1}{p_0 + p_1}\right] \tag{3.26}$$

here g_e is the generation rate arising from external illumination.

If we assume steady-state condition, $n_0/(n_0+n_1) = p_1/(p_0+p_1)$ and $p_1 n_1 = p_0 n_0$, following expression results

$$g_e = \frac{\Delta n}{\tau_n} = \frac{\Delta p}{\tau_p} = \frac{\Delta n p_0 + \Delta p n_0 + \Delta n \Delta p}{\tau_{n_0}(p_0 + p_1 + \Delta p) + \tau_{p_0}(n_0 + n_1 + \Delta n)} \tag{3.27}$$

If the trapping of the carriers by the trap/recombination centres is negligible in compare to the excess carrier densities, and hence Δn = Δp, the above equation will lead to the standard SRH recombination lifetime

$$\tau_{SRH} = \frac{\tau_{n_0}\left(p_0 + p_1 + \Delta p\right) + \tau_{p_0}\left(n_0 + n_1 + \Delta n\right)}{n_0 + p_0 + \Delta n} \tag{3.28}$$

3.5.4 SURFACE RECOMBINATION

The surfaces or interfaces of a silicon substrate represent a severe discontinuity in its crystalline structure. The large numbers of partially bonded silicon atoms give rise to many dangling bonds, and therefore, a large density of defect levels are found within the band gap near the semiconductor surface. Even if the silicon surface is not bare, say due to a native oxide, the presence of silicon-oxygen bonds can stress the crystal structure at the surface, which again introduces many defect states.

Surface recombination is a special case of SRH recombination in which localised states occur at the surface. The basic difference between surface recombination and SRH recombination is that in SRH recombination localised states occupy a single energy level within the band gap, where in case of surface recombination the localised states form a set of states and distributed across the band gap. Although the recombination principles are identical to SRH recombination, surface recombination is analysed in terms of surface recombination velocity (SRV) instead of lifetime.

The SRH analysis of section 3.5.3 again applies, although it has to be reformulated in terms of recombination events per unit surface area, rather than per unit volume.

For a single defect at the surface, the rate of surface recombination, U_S, is given by [43]

$$U_S = \frac{n_S p_S - n_i^2}{\frac{n_S + n_1}{S_{p_0}} + \frac{p_S + p_1}{S_{n_0}}} \tag{3.29}$$

where n_S and p_S are the concentrations of electrons and holes at the surface, and S_{p_0} and S_{n_0} are related to the density of surface states per unit area, N_{ts}, and the capture cross-sections, σ_n and σ_p, for the specific defect [43]

$$S_{n_0} = \sigma_n \nu_{th} N_{ts} \qquad and \qquad S_{p_0} = \sigma_p \nu_{th} N_{ts} \tag{3.30}$$

In reality, defect levels are so numerous that they can be considered to be continuously distributed throughout the band gap, and both their density and capture cross-sections will be dependent on their energy level. Using D_{it} for the density of interface traps at a given energy (rather than N_{ts} for a specific energy level) and integrating over the entire band gap, it follows that [43]

$$U_S = \int_{E_V}^{E_C} \frac{\nu_{th}\left(n_S p_S - n_i^2\right)}{\frac{n_S + n_1}{\sigma_p} + \frac{p_S + p_1}{\sigma_n}} D_{it} dE \tag{3.31}$$

The *surface recombination velocity*, S, is defined as

$$S = \frac{U_S}{\Delta n_S} = \int_{E_V}^{E_C} \frac{\left(n_0 + p_0 + \Delta n_S\right)\nu_{th} D_{it}}{\left(n_0 + n_1 + \Delta n_S\right)\sigma_p^{-1} + \left(p_0 + p_1 + \Delta n_S\right)\sigma_n^{-1}} dE \tag{3.32}$$

3.5.5 EMITTER RECOMBINATION

Emitter recombination refers to the carrier decay inside the emitter region and its surface as well. Emitter regions are heavily doped and hence, Auger recombination is very pronounced in these regions. To model emitter recombination several factors have to be taken into account, such as semiconductor degeneracy in emitter region, band gap narrowing, free carrier absorption, presence of dead layers, and diffusion related SRH defects. All these effects strongly vary with dopant densities with depth. However, Auger processes get exacerbated by the large number of minority carriers there by strongly absorbed high energy photons. Quality of the surface

passivation plays the significant role to circumvent the recombination in emitter regions. The effective recombination lifetime due to emitter can be written as [6]

$$\tau_{emitter} = \frac{qn_i^2 W}{J_{oe}\left(N_{dop} + \Delta n\right)} \tag{3.33}$$

here J_{oe} is the emitter saturation current density which incorporates both the surface bulk recombination in emitter.

CHAPTER 4

MODELLING MINORITY CARRIER LIFETIME IN MULTICRYSTALLINE SILICON

4.1 NECESSITY OF CARRIER LIFETIME MODELLING

The concepts of carrier lifetime in semiconductor materials and average life expectancy in demography are similar. Like common mortals, electrons (and holes) die after some time and the average of this time is called the *minority carrier life time*. The rate at which they disappear or recombine, is given, in p-type material by $\Delta n/\tau$, where τ is the electron lifetime, and Δn is the excess electron concentration, which is essentially equal to the total electron population in most practical cases. In a steady-state situation the generation and recombination rates are perfectly balanced. When a typical 300 μm thick silicon wafer is illuminated by strong sunlight of irradiance 1000 mW/cm^2, electrons and holes are generated at a rate of $G_L = 9\times10^{18} cm^{-3}s^{-1}$ [44]

$$G_L = \frac{\Delta n}{\tau} \tag{4.1}$$

In a solar cell it is important to determine the electron population. Because the voltage of a solar cell is directly related to it and is given by [45]

$$V_{OC} = \frac{kT}{q}\left(\frac{\Delta n(N_A + \Delta p)}{n_i^2} + 1\right) \tag{4.2}$$

In addition, cell‟s output current is also related to the life time. This is because electrons take some time to travel across the silicon wafer and they reach the pn junction only if their life expectancy is long enough to complete the journey.

The lifetime indicates the quality of silicon material. This quality depends, primarily, on the growth process like FZ or CZ grown. Besides, lifetime can change when wafers are processed at

high temperature or subjected to certain treatments. It is, therefore, essential to model the carrier lifetime before going for rigorous experiments or to be ascertained about correctness of experimental results.

4.2 RECOMBINATION MECHANISMS AND CARRIER LIFETIME

Once the electron-hole pairs are generated by absorption in the silicon, they are exposed to several recombination mechanisms. These processes occur in parallel and the recombination rate is the sum of those individual processes. Different recombination mechanisms and the lifetime associated with them are discussed below. The theory is supported by simulation results too.

4.2.1 RADIATIVE RECOMBINATION LIFETIME

Radiative recombination is simply the direct annihilation of an electron-hole pair. It is the inverse process to optical generation, the excess energy being released mainly as a photon with energy close to that of the band gap. General expression for radiative recombination lifetime, τ_{rad} yields [3]

$$\tau_{rad} = \frac{1}{B(n_0 + p_0) + B\Delta n} \tag{4.3}$$

From Eq. (4.3), the common relationships for the radiative lifetime in *n*-type and *p*-type material under low injection ($\tau_{rad,li}$) and high injection conditions ($\tau_{rad,hi}$) can be determined:

$$\tau_{rad,li} = \frac{1}{BN_{dop}} \qquad and \qquad \tau_{rad.hi} = \frac{1}{B\Delta n} \tag{4.4}$$

From fig. 4.1, it can be seen that the radiative lifetime depends on the inverse of the carrier density. Therefore, τ_{rad} is constant at low injection, but then decreases and continues to decrease as the injection level increases.

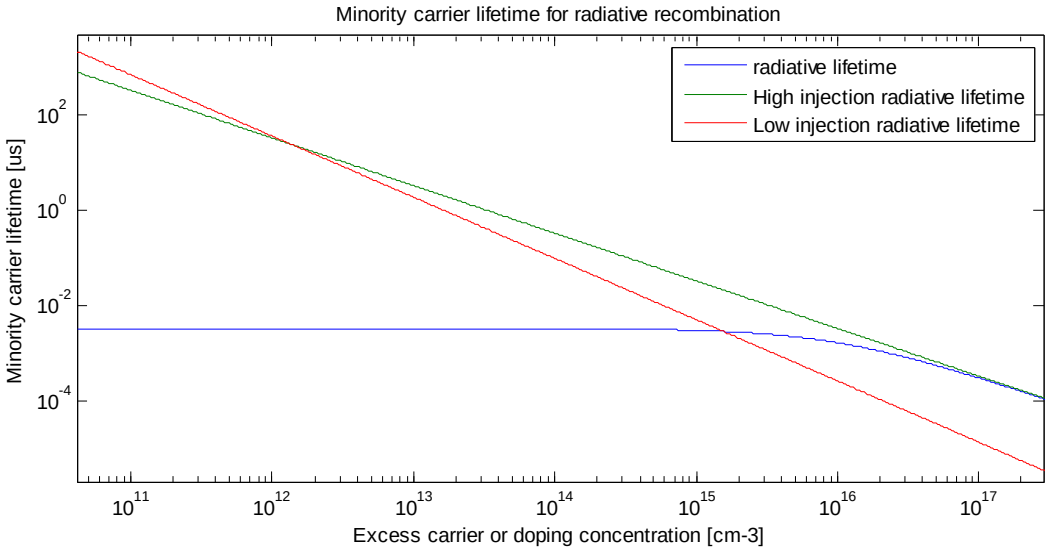

Fig. 4.1: Radiative recombination lifetime.

While radiative recombination is typically the dominant recombination process in direct semiconductors, where it forms the basis for the operation of light-emitting diodes, it is considered to be small or even negligible compared to other recombination processes in indirect semiconductors such as silicon.

4.2.2 AUGER RECOMBINATION LIFETIME

In Auger recombination, a collision between two similar carriers results in the excitation of one carrier to a higher kinetic energy, and the recombination of the other across the band gap with a carrier of opposite polarity. The extra energy will be lost as heat as the excited carrier relaxes to the band edge. Using the effective auger coefficients, the injection dependent CE-Auger life time may be calculated from Equation 3.21 of chapter 3.

The Auger lifetime ideally depends on the inverse of the carrier density squared and this can be better explained by the fig. 4.2. It shows a stronger dependence with the injection level than τ_{rad}, and therefore, Auger recombination will become the dominant mode of recombination in silicon for high injection levels, as might occur in concentrator solar cells, or for high dopant densities, as occurs in heavily doped emitter regions of silicon solar cells.

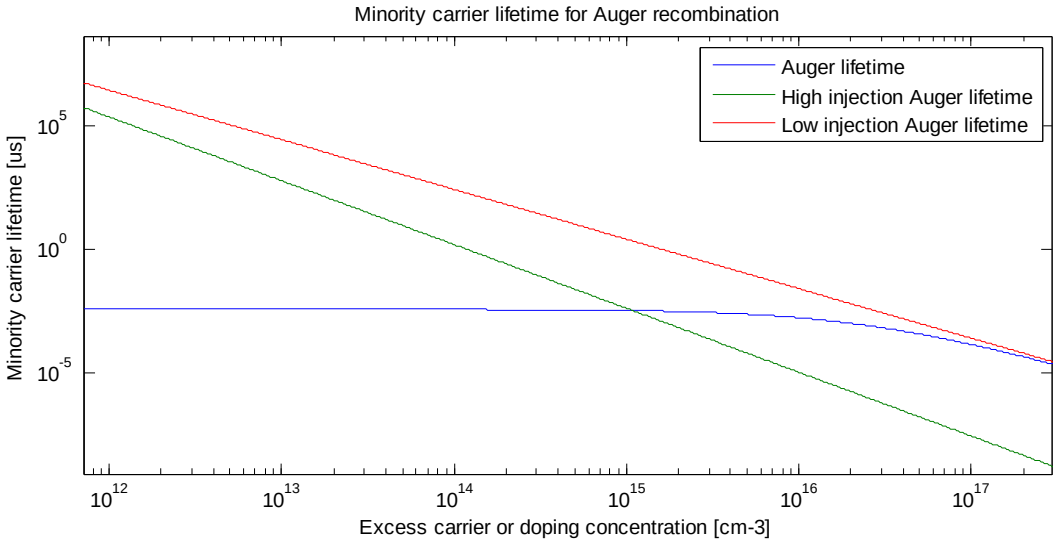

Fig. 4.2: Auger Recombination lifetime.

4.2.3 EFFECTIVE INTRINSIC RECOMBINATION LIFETIME

Intrinsic recombination lifetime comprises of the summation of radiative recombination lifetime and auger recombination life, and is given as

$$\frac{1}{\tau_i} = \frac{1}{\tau_{rad}} + \frac{1}{\tau_{Auger}} \tag{4.5}$$

For low injection level,

$$\frac{1}{\tau_{i,lli}} = \frac{1}{\tau_{rad,lli}} + \frac{1}{\tau_{Auger,lli}} \tag{4.6}$$

For high level injection

$$\frac{1}{\tau_{i,hli}} = \frac{1}{\tau_{rad,hli}} + \frac{1}{\tau_{Auger,hli}} \tag{4.7}$$

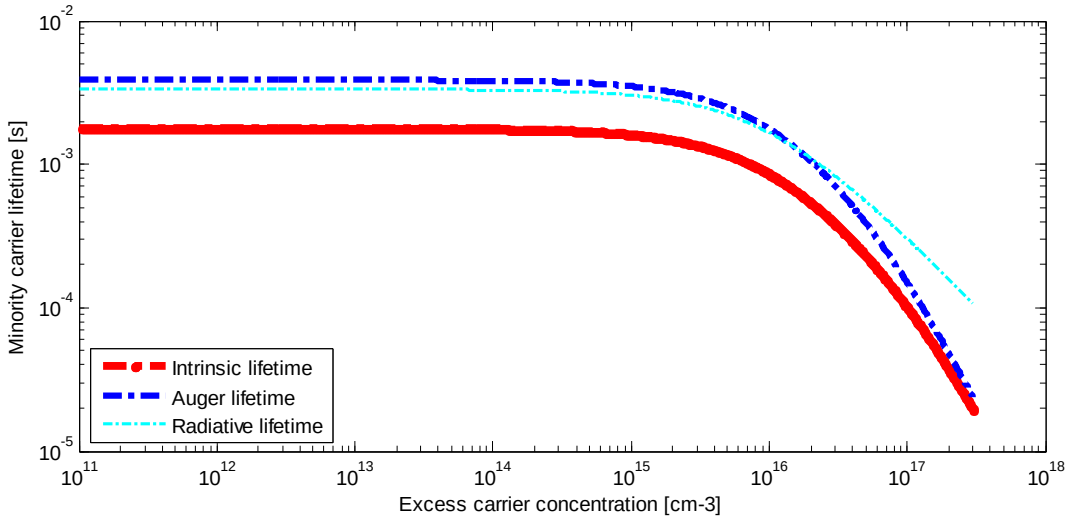

Fig.4.3: Intrinsic recombination lifetime.

Fig. 4.3 - 4.5 shows the intrinsic recombination lifetime for minority carrier for low and high injection level. At high injection level, intrinsic lifetime is dominated by the Auger recombination as expected from the theory. At low injection, intrinsic recombination lifetime shows strong dependence on the doping concentration.

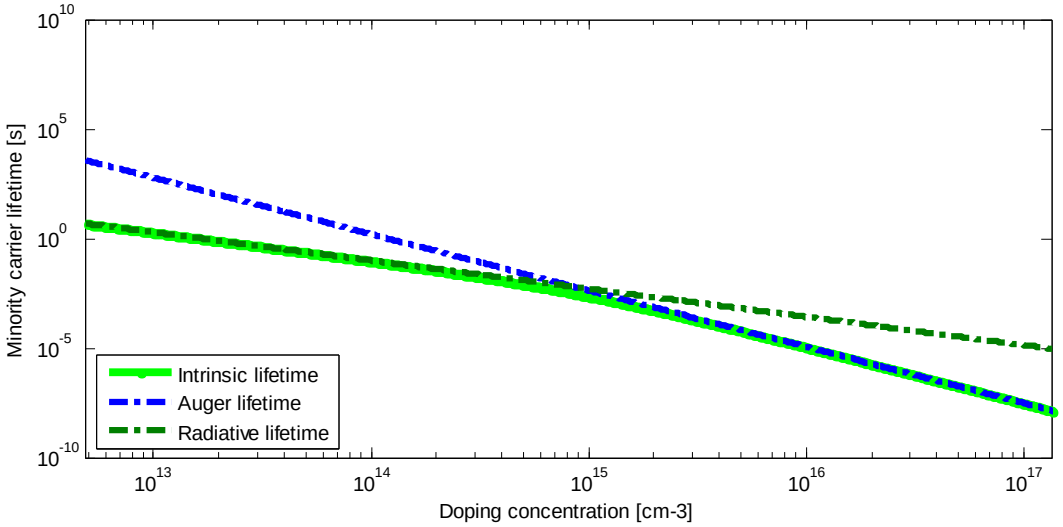

Fig.4.4: Intrinsic recombination lifetime of minority carrier for low injection level

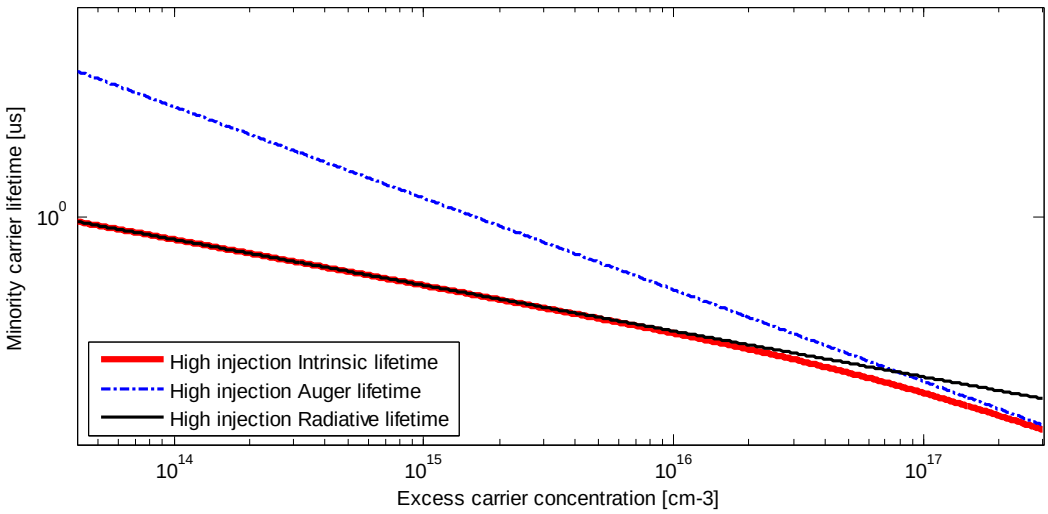

Fig. 4.5: High injection level intrinsic recombination lifetime.

4.2.4 SHOCKLEY-READ-HALL RECOMBINATION LIFETIME

SHR recombination lifetime can be modelled using the Equation 3.28 of chapter 3. The simulated result is shown in fig. 4.6. It can be seen that the SRH lifetime is constant for low level injection densities where it increases quadratically for high injection level. An important result follows from Eq. 3.28 is that the traps with energies close to the centre of the band gap (deep defects) are the most effective recombination centres.

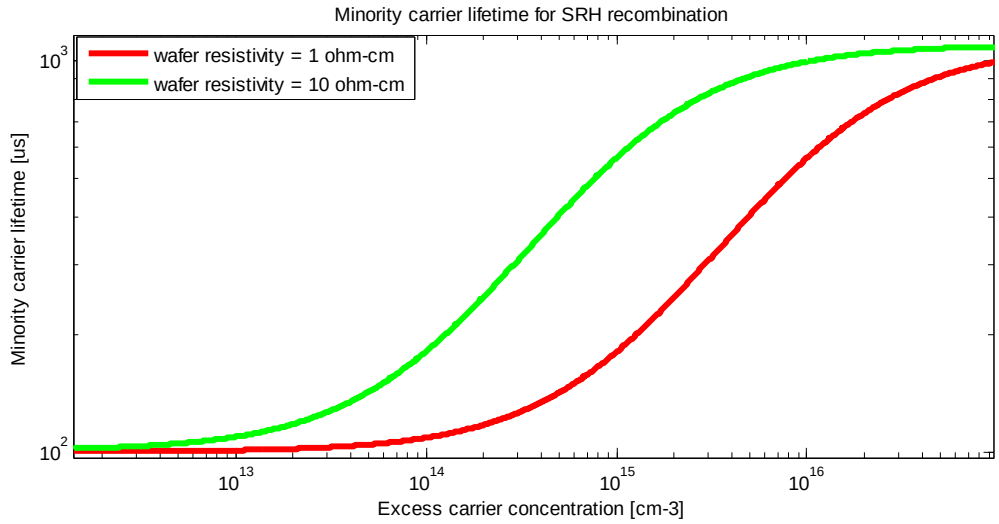

Fig. 4.6: SRH recombination lifetime of minority carrier in silicon wafer of two different resistivity.

4.2.5 BULK RECOMBINATION LIFETIME

There are at least three recombination mechanisms are associated with a given multicrystalline silicon sample, namely, radiative recombination, Auger recombination and SRH recombination. The bulk lifetime is the sum up of these three recombination lifetime.

$$\frac{1}{\tau_{bulk}} = \frac{1}{\tau_i} + \frac{1}{\tau_{SRH}} \tag{4.8}$$

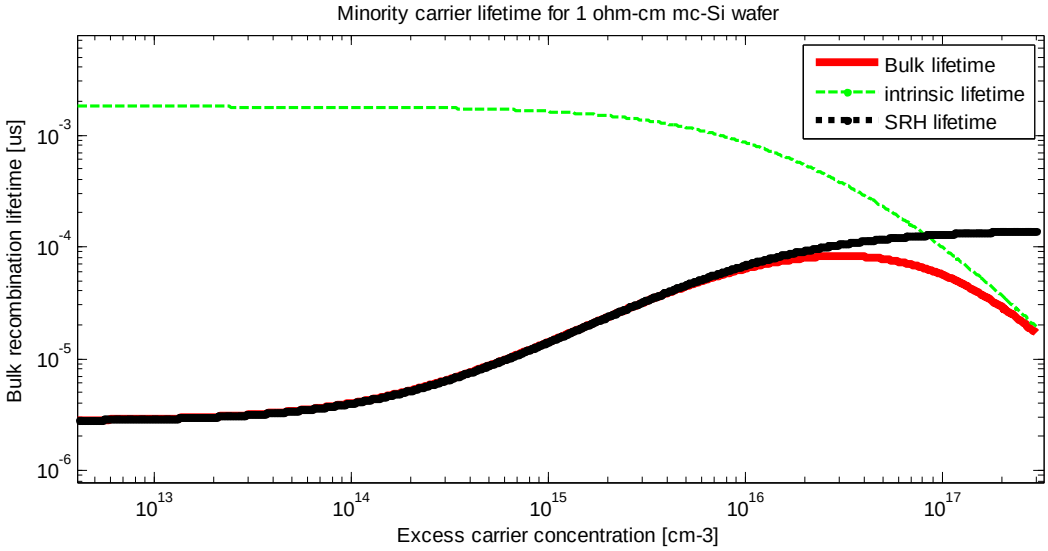

Fig. 4.7: Bulk recombination lifetime of minority carrier in silicon.

Fig. 4.7 shows that at low injection level, bulk lifetime is dominated by the SRH lifetime while at high injection level (>10^{17}), it is dominated by the Auger recombination lifetime.

4.2.6 EMITTER RECOMBINATION LIFETIME

Quality of the emitter plays a significant role in the conversion efficiency of the silicon solar cell. Emitter is essentially used to collect the photogenerated minority carriers. Sometimes it provides passivation effect at the semiconductor surface. Optically generated carriers come from the base then recombine with the dopant atoms in emitter at the space-charge region, volume or surface of the emitter. The effective recombination lifetime due to the emitter can be written as [6]

$$\tau_{emitter} = \frac{qW}{J_{0e}} \frac{n_i^2}{N_A + \Delta n} \tag{4.9}$$

At low injection with respect to base

$$\tau_{emitter,lli} \cong \frac{qW}{J_{0e}} \frac{n_i^2}{N_A} \tag{4.10}$$

At high injection

$$\tau_{emitter,hli} = \frac{qW}{J_{0e}} \frac{n_i^2}{\Delta n} \tag{4.11}$$

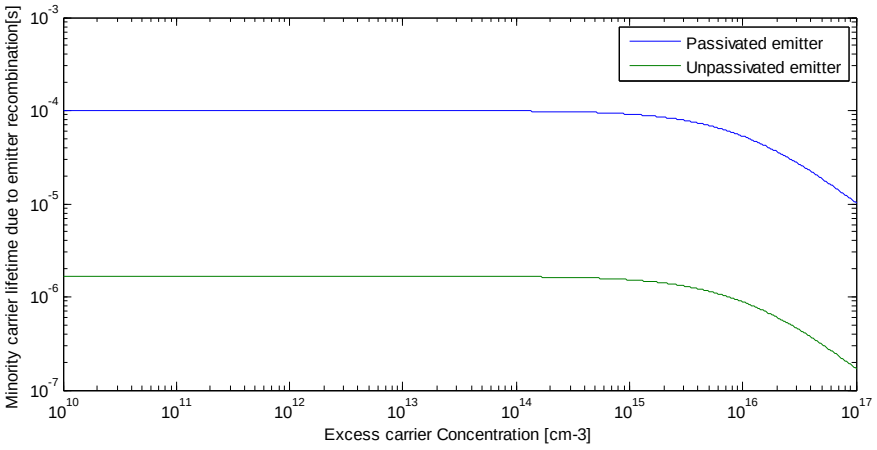

Fig. 4.8: Effective emitter recombination lifetime of minority carrier.

Fig. 4.8 shows the effective emitter recombination lifetime and the impact of emitter saturation current density on the minority carrier lifetime. It is obvious that the quality of surface passivation has substantial impact on the total recombination attributed to the emitter region.

4.2.7 SURFACE RECOMBINATION LIFETIME

The surface recombination velocity, S is typically used for quantifying surface recombination processes. Surface recombination lifetime is given as [46]

$$\tau_{surface} = \left(\frac{2S}{W} + \frac{1}{D_n} \left(\frac{W}{\pi} \right)^2 \right)^{-1} \tag{4.12}$$

Fig. 4.9 and 4.10 shows the impact of wafer thickness and surface recombination velocity (SRV) on the variation of minority carrier lifetime. It is obvious that surface recombination velocity is the highest on the top of the surface of the wafer while it decreases sharply along the deeper into the wafer. As expected, a reciprocal relationship between the minority carrier lifetime and SRV or wafer thickness, respectively, is generally observed from the simulated results. Detailed knowledge of the surface properties of the Si wafers will help to choose the best or to explore the new passivation techniques to circumvent the minority carrier lifetime deterioration due to the SRV and dangling bonds over the semiconductor surfaces.

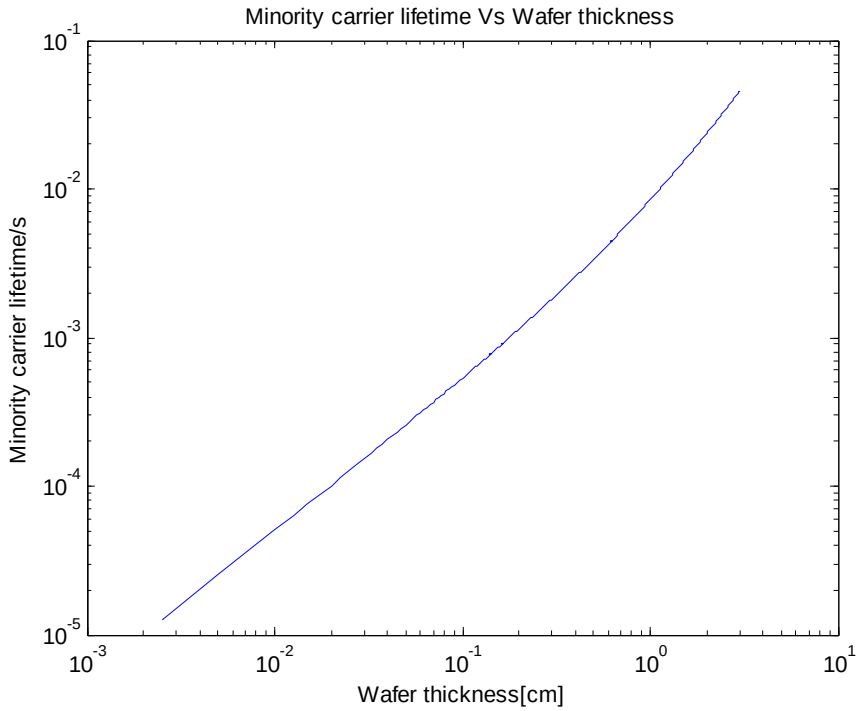

Fig.4.9: Variation of minority carrier lifetime with respect to wafer thickness.

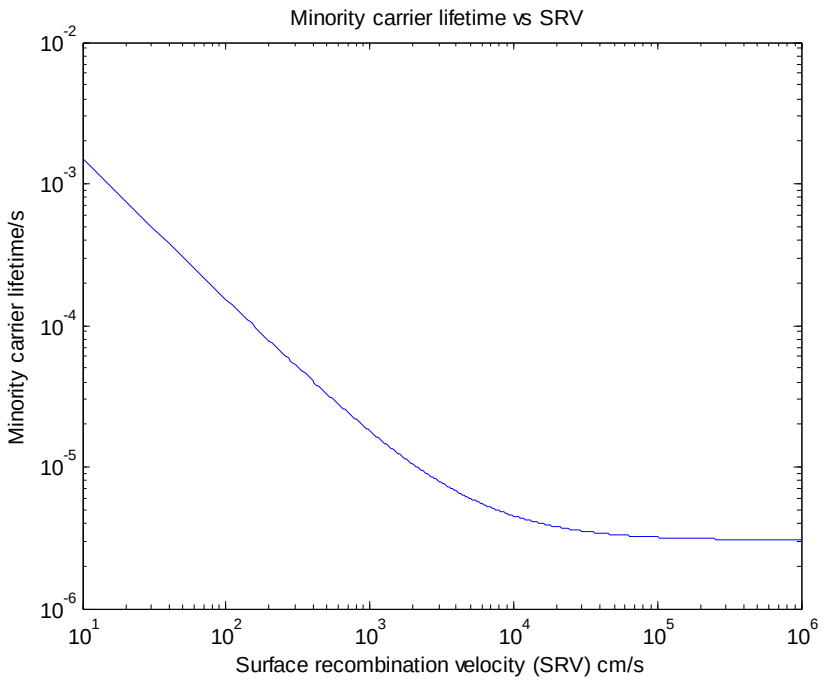

Fig. 4.10: Variation of minority carrier lifetime with respect to surface recombination velocity.

4.2.8 EFFECTIVE RECOMBINATION LIFETIME

The recombination lifetime discussed above may occur simultaneously in a given sample. For an independent process the overall recombination rate is just sum of the individual recombination rates, resulting in an effective lifetime τ_{eff} given by

$$\frac{1}{\tau_{eff}} = \left(\frac{1}{\tau_{SRH}} + \frac{1}{\tau_{Auger}} + \frac{1}{\tau_{rad}} \right) + \frac{1}{\tau_{surface}} + \frac{1}{\tau_{emitter}} \tag{4.13}$$

The simulated results that shown in fig.4.11 shows that the effective lifetime is dominated by bulk recombination process rather than intrinsic recombination mechanisms. The lifetime increases with injection level for SRH recombination through deep defects but decreases for intrinsic bulk recombination processes. The resulting effective lifetime is, therefore, dominated by SRH recombination at low injection and Auger recombination at high injection. As mc-Si riches with numerous crystal defects that act as defect centres for SRH recombination, minority carrier lifetime in mc-Si solar cell is much lower than that of mono-crystalline silicon solar cell.

This is one of the vital reasons why solar cells made from mono-Si wafers have higher energy conversion efficiency compare to mc-Si.

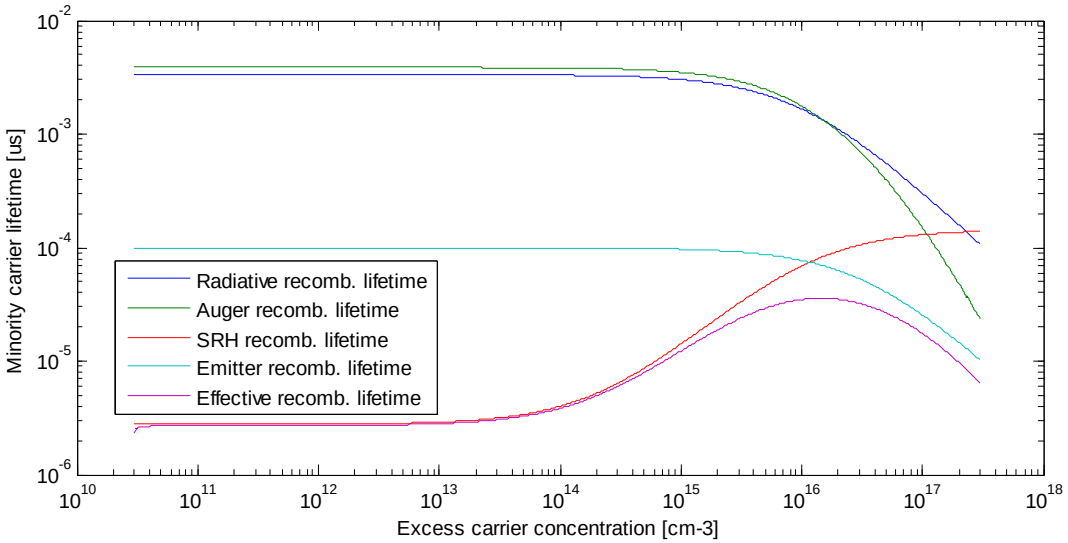

Fig. 4.11: Effective recombination lifetime of minority carrier.

4.3 CONCLUSION

To ensure an accurate interpretation of the recombination lifetime, the principle recombination mechanisms in silicon have been studied analytically. The parameters for modeling are taken from published literatures. Recombination greatly reduce the effective carrier lifetime, hence, therefore, reduces the performance of solar cells, particularly the cell voltage and efficiency. Indeed, it has been concluded that of the avoidable losses in silicon solar cells, recombination losses are the most significant for both high efficiency laboratory cells and commercial multicrystalline cells.

CHAPTER 5

ANALYTICAL MODELLING OF MINORITY CARRIER LIFETIME OF INTENTIONALLY Fe CONTAMINATED MC-Si SOLAR CELLS

5.1 INTENTIONAL CONTAMINATION OF Fe IN Si

Deliberate contamination of Fe in silicon is assumed to make through the crystal growth process of silicon and will remain dissolved and electrically active within the whole contaminated crystal. The concentration of dissolved Fe can be directly calculated from the metal quantity weighed into the melt using the segregation coefficients of Fe [47]. Here axial variation of Fe concentration is neglected and assume uniform over a typical wafer thickness cut from the crystal.

5.2 IMPACT OF Fe ON SRH RECOMBINATION LIFETIME

Iron (Fe) has been identified as critical impurities concerning their electrically active incorporation in the silicon lattice. Iron precipitates at the extended defects of mc-Si, forms electrically active energy levels within the band gap, serves as trap or recombination centre, and is generally considered as unfavorable for minority carrier lifetime.

Electronic performance of a solar cell is greatly influenced by the one or more of the recombination mechanism for a particular cell design or substrate type. When Fe presents in silicon, SRH recombination become predominant mechanism for minority carrier lifetime and is the primary determinant of the open circuit voltage achievable in a solar cell. So information obtained through analytical modelling of intentionally Fe incorporated mc-Si solar cell will become useful in allowing further research efforts to be focused in the appropriate areas of cell design and fabrication.

SRH recombination lifetime depends on the impurity concentration (here, Fe, for example), energy level introduced by the impurity within the band gap, capture cross section of electron

and hole in the defect energy states, and fundamental capture time constants of electron and hole. The SRH lifetime described in chapter 3 is modified here for both low injection and high injection of excess carrier to get better insight of the effect of the interstitial iron [Fe_i] contamination.

Following the standard SRH lifetime equation, the injection independent SRH lifetime is given as

$$\tau_{SRH,lli} = \frac{1}{p_0 + n_0}\left[\tau_{n0}\left(p_0 + p_1\right) + \tau_{p0}\left(n_0 + n_1\right)\right] \tag{5.1}$$

Equation 5.1 is further simplified for p-type and n-type semiconductor, respectively

$$\tau_{SRH,lli} = \frac{1}{p_0}\left[\tau_{n0}\left(p_0 + p_1\right) + \tau_{p0} n_1\right] \text{ for p-type} \tag{5.2}$$

$$\tau_{SRH,lli} = \frac{1}{n_0}\left[\tau_{n0} p_1 + \tau_{p0}\left(n_0 + n_1\right)\right] \text{ for n-type} \tag{5.3}$$

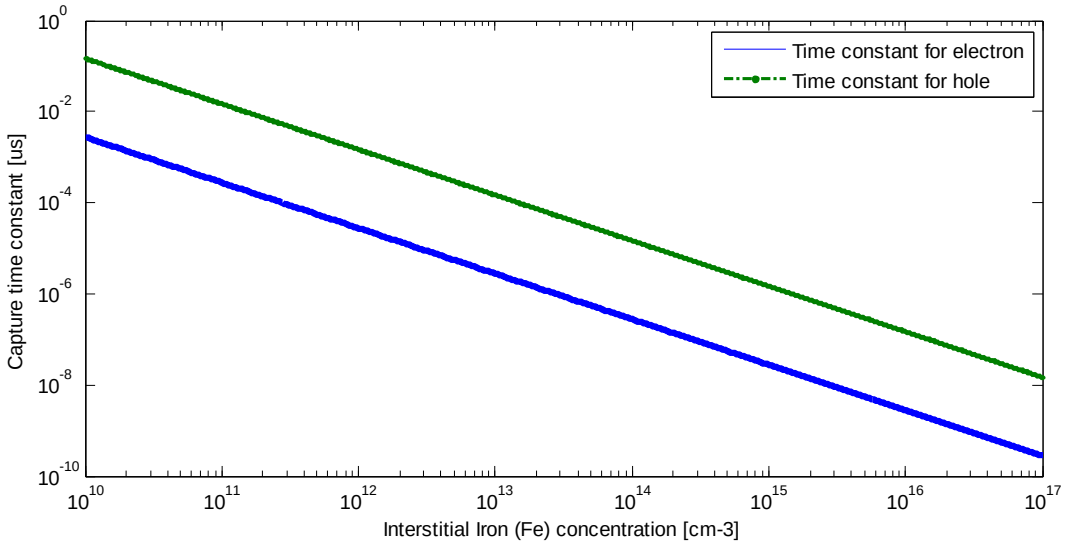

Fig. 5.1: Fundamental time constants for electron and hole as a function of [Fe_i].

Fig. 5.1 shows the fundamental capture time constants for both electron and hole as a function of interstitial iron concentration. Fig. 5.2 shows the effect interstitial iron and capture time constant

on the injection independent SRH lifetime of minority carrier for both n-type and p-type silicon solar cells, respectively. Both of the curves show a linear decrease in lifetime values for an increase in interstitial iron concentration. The carrier capture cross sections for electron and hole are taken as 3.6×10^{-15} and 6.8×10^{-17}, respectively [6]. Low capture time constant of electron than hole indicates that the when electron will get captured due to Fe related trap centers, it will get back faster than hole to the respective band from where it comes and trapped.

In the presence of [Fe_i], n-type wafer shows less prone to SRH recombination lifetime than that of its counterpart p-type wafer. The higher lifetime for n-type wafers is primarily due to the shorter capture period for electron. It may also be inferred that iron in n-type wafer has greater influence as trap centre rather than recombination centre and vice-versa for p-type. This result suggests that solar cells made out of n-type wafer will have higher conversion efficiency than p-type. But other tertiary effects should be taken into account before go for a particular wafer type to make solar cell device.

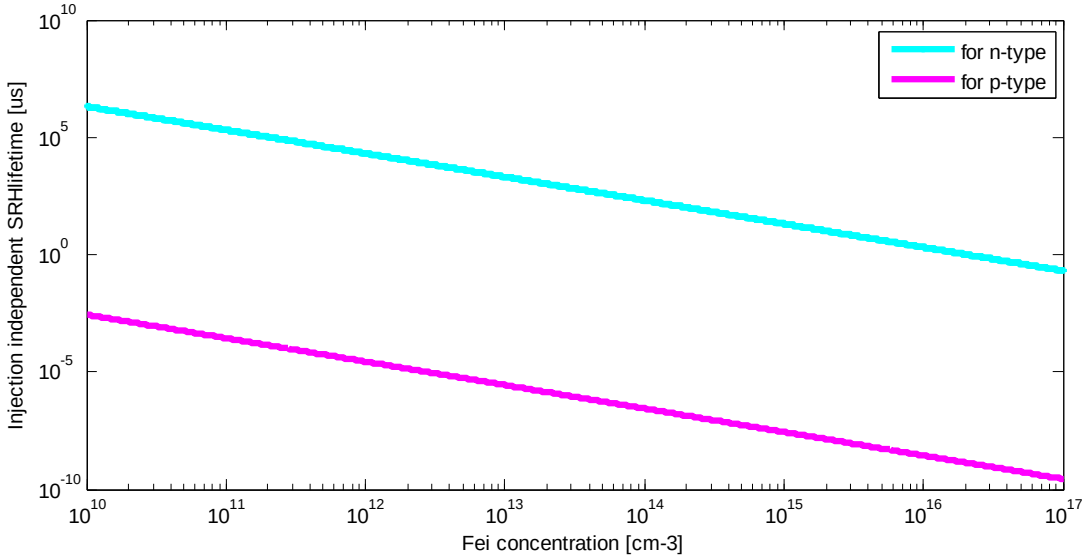

Fig. 5.2: Injection independent SRH lifetime of minority carrier for varying [Fe_i].

At high injection level, SRH lifetime is independent of the defect level. So our concerns are on low injection SRH lifetime.

5.2.1 RECOMBINATION STRENGTH OF Fe AT LOW INJECTION LEVEL

The recombination over a deep defect state is limited by the capture of minority carrier at low injection level. Because for a mid-gap trap, $n_1 = p_1 = n_i$ are very smaller than doping concentration. As a result, $\tau_{SRH,lli} \cong \tau_{n0}$ for p-type doping and $\tau_{SRH,lli} \cong \tau_{p0}$ for n-type doping. This is the reason why injection independent SRH lifetime is often called minority carrier lifetime.

Minority carrier capture time constant is the absolute minimum of SRH lifetime and serves as scaling factor of the SRH lifetime. The normalization of SRH lifetime by minority carrier capture time constant is a direct measure of the strength of the recombination activity of a particular defect.

There are three defect energy levels, namely, deep level, shallow level and transition level may possible for an impurity presents in mc-Si. A deep level defect energy level lies at the middle of silicon band gap energy, shallow level defect lies close to VB for hole and close to CB for electron, transition energy level lies in lower half of band gap for hole and in upper half for electron.

For the following calculation of the recombination strength of Fe, the relevant data will be taken from the table 5.1 and 5.2.

Table 5.1: Fit parameter for SRH recombination [6]

Dopant density (cm^{-3})	Wafer thickness (cm)	J_{0e}(A/cm^2)	N_t(cm^{-3})	τ_{n0} (s)	τ_{p0} (s)
1.5×10^{16}	0.003	1.9×10^{-13}	9×10^{12}	3.33×10^{-5} 1.09×10^{-4}	1.11×10^{-2} 1.09×10^{-3}

Table 5.2: Energy levels and capture cross section of Fe.

Recomb. centre	Energy level, E_t (eV)	σ_n (cm^{-2})	σ_p (cm^{-2})	Reference
Fe_i	$E_V + 0.38$	5×10^{-14}	7×10^{-17}	[36]
FeB acceptor	$E_C - 0.23$	3×10^{-14}	2×10^{-15}	[6, 36]

The normalized low injection-SRH lifetime can be obtained from equations 5.2 and 5.3, such as

$$\frac{\tau_{SRH,lli}}{\tau_{n0}} = \frac{1}{p_0}\left[p_0 + p_1 + \mathrm{X}n_1\right] \text{ for p-type} \tag{5.4}$$

$$\frac{\tau_{SRH,lli}}{\tau_{p0}} = \frac{1}{n_0}\left[n_0 + n_1 + \mathrm{X}^{-1}p_1\right] \text{ for n-type} \tag{5.5}$$

where, $\mathrm{X} = \frac{\tau_{p0}}{\tau_{n0}}$.

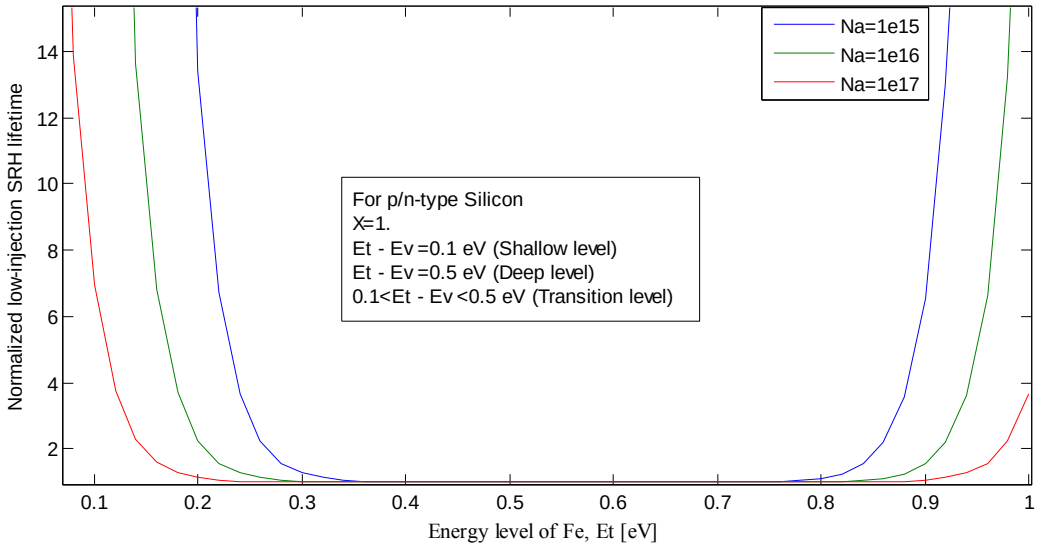

Fig 5.3: Recombination strength of Fe related defect states for symmetric capture cross section at 300^0K.

Fig. 5.3, 5.4 and 5.5 shows the recombination strength of Fe related defect centers in silicon. The simulated results are shown for three different energy levels (shallow, deep and transition) that might occurred in presence of an impurity in silicon. From fig. 5.3 and 5.5, it is shown for symmetric capture cross section of minority carriers that shallow level become recombination active for higher doping concentration, deep level exhibits maximum recombination activity over the whole doping concentration, and recombination activity of transition level shows strong dependence on doping concentration for low-injection SRH lifetime. It was shown in Fig. 5.4 that for a defect energy level E_t, smaller the symmetry factor X and therefore higher the relative capture time-constant for electron, the more effective is the defect for recombination and therefore the smaller is the low-injection normalized SRH lifetime.

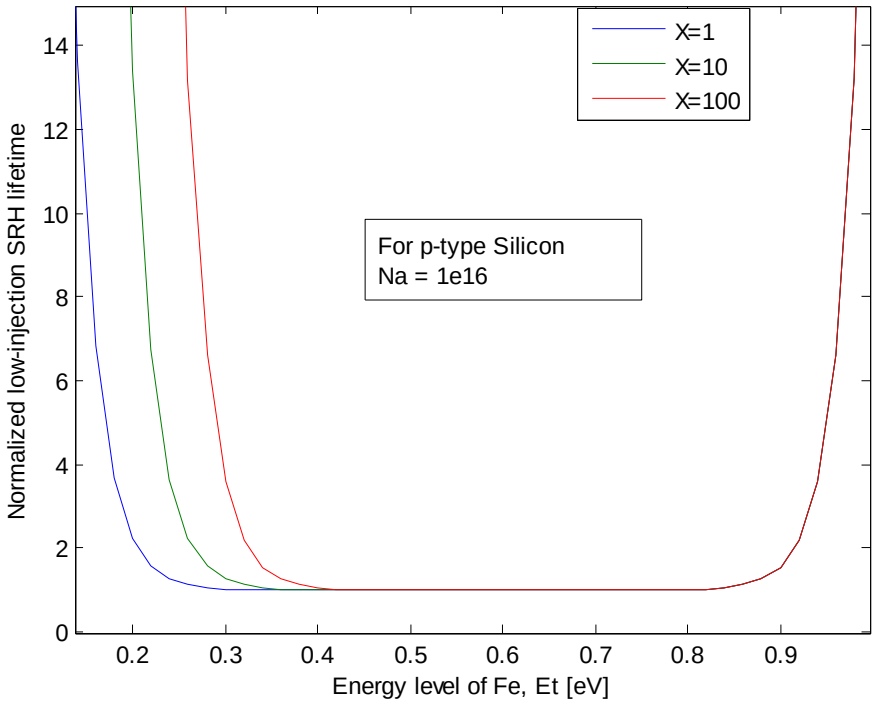

Fig 5.4: Recombination strength of Fe related defect states for asymmetric capture cross section at 300^0K.

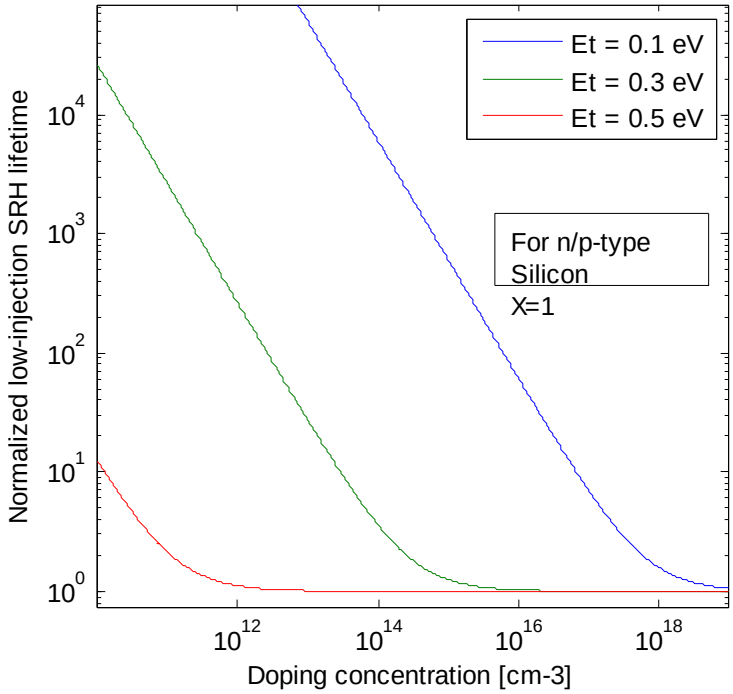

Fig.5.5: Impact of doping concentration for Fe with different energy levels.

5.2.2 INFLUENCE OF Fe ON TEMPERATURE DEPENDENT NORMLAIZED SRH LIFETIME

If we assume an iron related defect energy level at the upper half of the band gap, Equation 5.4 reduces to

$$\frac{\tau_{SRH,lli}}{\tau_{n0}} = \frac{1}{p_0}\left[p_0 + \mathrm{X}n_1\right] \text{ for p-type} \tag{5.6}$$

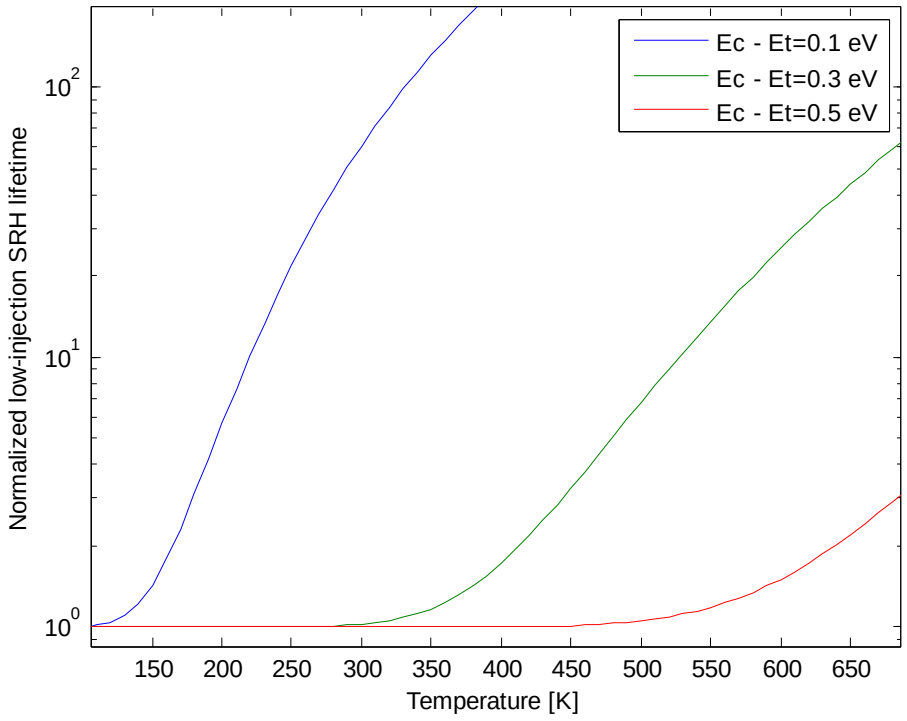

Fig. 5.6: Impact of Fe related defect energy levels on T-dependent low-injection normalized SRH lifetime for symmetric capture cross-section and fixed doping of 10^{16} cm^{-3}.

To incorporate the temperature dependence, n_1 and τ_{n0} should be modified as follows

$$\tau_{n0}(T) = \tau_{n0}^{300K}\left(\frac{T}{300K}\right)^{-1/2} \tag{5.7}$$

And

$$n_1(T) = N_C^{300K}\left(\frac{T}{300K}\right)^{3/2}\exp\left(-\frac{E_C - E_F}{KT}\right) \tag{5.8}$$

The overall T-dependent low-injection normalized SRH lifetime then become

$$\frac{\tau_{SRH,lli}}{\tau_{n0}(T)} = \frac{1}{p_0}\left[p_0 + \mathrm{X}n_1(T)\right] \text{ for p-type} \tag{5.9}$$

It can be seen from fig. 5.6 that at low temperature shallow level defect become less recombination active while deep level defect become most recombination active. Hence, shallow level defect shows an exponential increase in SRH lifetime. At higher temperature, s steep increase in SRH lifetime is observed. At higher T, $n_1(T)$ in Equation 5.9 dominates and the Fermi energy level approaches to mid-gap, hence a decrease in recombination activity of deep level defect results in.

5.3 CONCLUSION

Shockley-Read-Hall (SRH) recombination is the main determinant for the effective minority carrier lifetime in silicon. This research has focused on the study to find the recombination strength of interstitial iron on low injection Shockley-Read-Hall (SRH) recombination in compensated solar grade silicon by means of analytical modelling. This study found that strength of iron in SRH recombination is depends on the doping concentration and symmetry of minority carrier capture cross-section. This study shows that iron become more recombination active at higher doping and at lower symmetry of capture cross-section.

CHAPTER 6

MINORITY CARRIER LIFETIME OF Fe CONTAMINATED COMPENSATED SOLAR-GRADE-SILICON

6.1 INTRODUCTION

Fast diffusion of solar PV requires the cost level cut down to acceptable minimum so that it can meet the grid parity of conventional electricity. Among several approaches to reach this goal, using inexpensive low-grade silicon, such as solar grade silicon (SoG), is a way to minimize the cost of solar cells production. Based on the purity, three kinds of silicon are available, namely metallurgical grade (98% pure), solar grade (99.9999% pure) and electronic grade (99.9999999% pure) silicon. The metallurgical silicon is not suitable for PV application. Although there might have slight differences in performance with compare to EG Si, solar grade (SoG) silicon is the optimal choice to cut-down the cost up-to acceptable minimum as it is the cheapest among the three types of above mentioned graded silicon.

This low-cost SoG material often contain high concentration of unwanted dopant species such as B, P and Al. These doping species introduce energy levels in the Si bandgap in the vicinity of the conduction band (E_C) for donor atoms (i.e. P) or in the vicinity of the valence band (E_V) for acceptor atoms (i.e. B).These energy levels enhance the trapping of the free carriers and responsible for low minority carrier lifetime due to Shockley-Read-Hall (SRH) recombination [6]. Due to have their higher segregation coefficient, the complete removal of electrically active impurities boron (B) and phosphorus (P) using conventional purification techniques, such as Siemens process, are quiet challenging, meaning that SoG is often compensated. Both B and P introduce shallow energy levels (B at Ev+0.045 eV and P at Ec-0.044 eV) [48] near the energy bands and act as either recombination or trap centres. These shallow energy levels enhance the recombination lifetime of minority carrier.

Previous works have determined the maximum concentrations of dopants that can be tolerated in the SoG feedstock without an excessive loss in the efficiency of the resulting solar cells, and have demonstrated the solar cell performance on compensated material that might be comparable

with noncompensated solar cells [49,50]. Recent studies explain the transport properties and impact of boron-oxygen related defect in compensated silicon [51-53]. Dubois et al. [50] studied the effect of compensation level on carrier life time. Very recently Macdonald and Cuevas [54] studied the recombination in compensated silicon for solar cells. Previous studies showed that compensation would lead to increase in carrier scattering mechanism, lower the carrier mobilities, and hence could limit the lifetime in highly doped SoG Si specially after phosphorus diffusion step [55]. This study finds that it is possible to increase both the intrinsic and SRH recombination lifetime of minority carrier significantly by virtue of suitable boron-phosphorus compensation.

The compensation in p-Si was done with phosphorus (P) for PV applications and it was assumed that cell is intentionally contaminated by interstitial iron, Fe_i. [Fe_i] equals to defect density N_t which acts as trap/recombination centre for SRH recombination.

6.2 ENHANCEMENT OF CARRIER LIFETIME DUE TO COMPENSATION

There is a direct correlation between the carrier lifetime and conversion efficiency of solar cell [6].Extensive research endeavor was put over the last few decades to ameliorate the adverse factors of lifetime killer to upgrade the efficiency of both single doped mono and multi-crystalline silicon solar cells. We have deployed those previously published relevant data to study the impact of compensation on minority carrier lifetime. By „lifetime" we have meant recombination lifetime due to the results of radiative, Auger and SRH recombination processes [3].

This study uses the analytical equations available for different recombination mechanisms at low injection and low temperature [3,6]. The equations are slightly modified to incorporate the compensation effect. The presence of interstitial iron introduced defect centre at the energy level Ev + 0.38 eV. Iron-boron pair introduced energy level at Ec - 0.23 eV and Ec - 0.29 eV [36]. These energy levels are mainly responsible for SRH recombination [7-8]. Compensation reduced the net doping concentration, and has great influences on intrinsic recombination processes [54].

6.2.1 IMPROVEMENT IN INTRINSIC RECOMBINATION LIFETIME

Intrinsic recombination comprised of radiative and Auger recombination. Radiative recombination is simply the direct annihilation of an electron-hole pair. It involves a conduction band electron falling from an allowed conduction band state into a vacant valence band state (a hole) .Traditionally, Auger recombination is viewed as a three-particle interaction where a conduction band electron and a valence band hole recombine, with the excess energy being transferred to a third free electron or hole. The charge carriers involved are assumed to be non-interacting quasi-free particles. Based on the experimental results, Kerr and Cuevas [50] developed a general expression for intrinsic recombination lifetime describing the combined effect of Auger and radiative recombination:

$$\tau_{\text{int}rinsic} = \frac{1}{(p_0 + n_0 + \Delta n)(1.8\times10^{-24} n_0^{0.65} + 6\times10^{-25} p_0^{0.65} + 3\times10^{-27}\Delta n^{0.8} + 9.5\times10^{-15})} \tag{6.1}$$

For the case of compensated p-type silicon ($N_A \succ N_D$), p_0 and n_0 in the equations have to be calculated by following equations

$$p_0 = \frac{N_A - N_D}{2} + \sqrt{\frac{(N_A - N_D)^2}{4} + n_i^2} \tag{6.2}$$

$$n_0 = \frac{n_i^2}{p_0} = \frac{n_i^2}{N_A - N_D} \tag{6.3}$$

For a fixed acceptor doping of $N_A = 10^{17}$ cm^{-3}, donor concentration, N_D is varied over a range of 10^{14} to 10^{16} so that it becomes predominantly p-type. Net hole concentration, p_0, for p-type compensated silicon is the difference of N_A and N_D.

At low injection, radiative recombination is inversely proportional to net doping while Auger recombination is inversely proportional to the square of the net doping. In uncompensated silicon net doping in p-type silicon is simply equal to N_A. In uncompensated silicon the impact of intrinsic recombination in carrier lifetime is negligible (shown in figure 6.1), but our simulated results showed it is not the same case for compensated silicon. There is a substantial increase (about 100 times) in minority carrier lifetime for low level compensation and is shown in fig.

6.2. Due to compensation of boron by phosphorus atoms, a reduction in free carrier shifts the Fermi level near the mid gap of energy band.

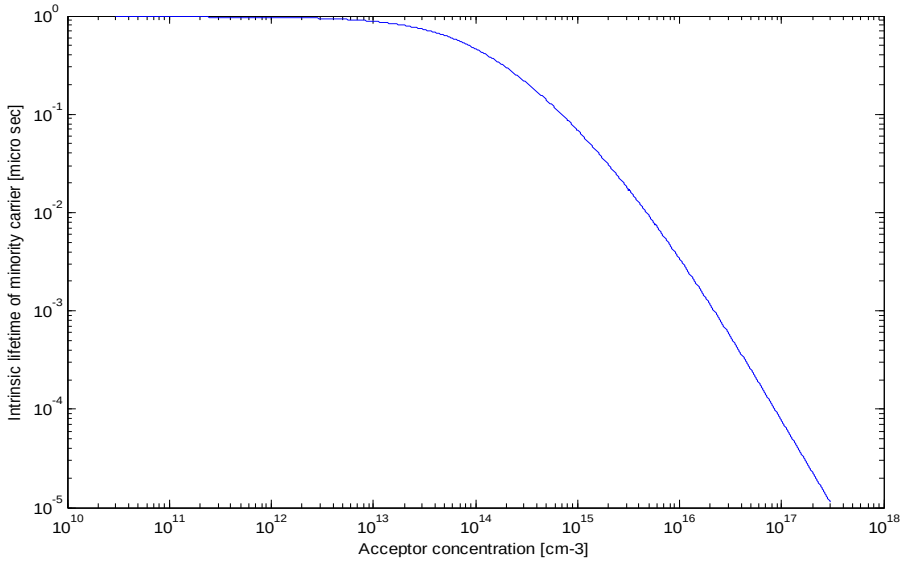

Fig. 6.1: Intrinsic carrier lifetime of minority carrier in uncompensated SoG Silicon.

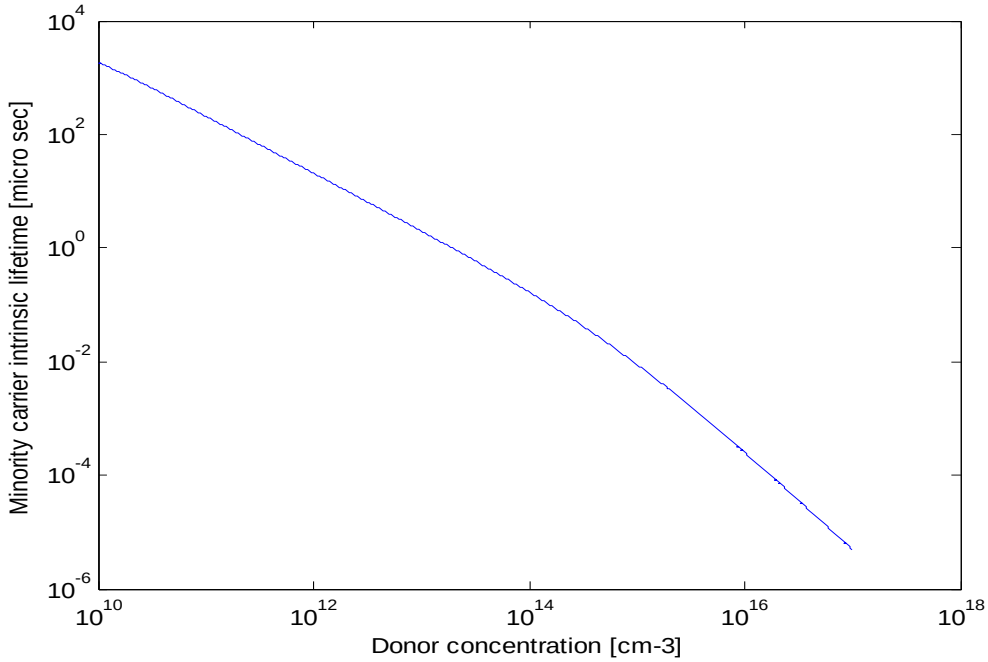

Fig. 6.2: Intrinsic carrier lifetime of minority carrier in donor compensated SoG Silicon.

As a result, the attractivity of neutral boron becomes exacerbated for the electrons. Coulomb interaction between quasi-free particles results local inhomogeneities in the carrier density and induces a spatial correlation of electron-hole pairs due to the formation of bound states. These bound states dominate under low doping concentration and found to be vanished at doping concentration above 10^{18} cm^{-3} because of complete screening of electron-hole interaction [40]. The overall impact is an increase in the minority carrier lifetime.

The compensation level, C_l is defined as N_D/N_A-N_D, N_A and N_D being the total concentrations of acceptor and donor species, respectively. In p-Si, it is considered fixed [B] equal to 3×10^{17} cm^{-3} and injection level equal to 10^{12} cm^{-3} while calculating intrinsic carrier lifetime. Although the intrinsic recombination lifetime in non-compensated silicon solar cell is almost negligible, from the simulated results, it has found a strong increase in intrinsic lifetime with C_l. Indeed, an absolute gain of 0.02 second is observed (shown in fig.6.3) for every decade change in C_l which is a huge for p-Si solar cell. This is due to a considerable reduction of the recombination strength of B. This predicted result could lead to strong improvements in the conversion efficiency of highly B doped solar cells.

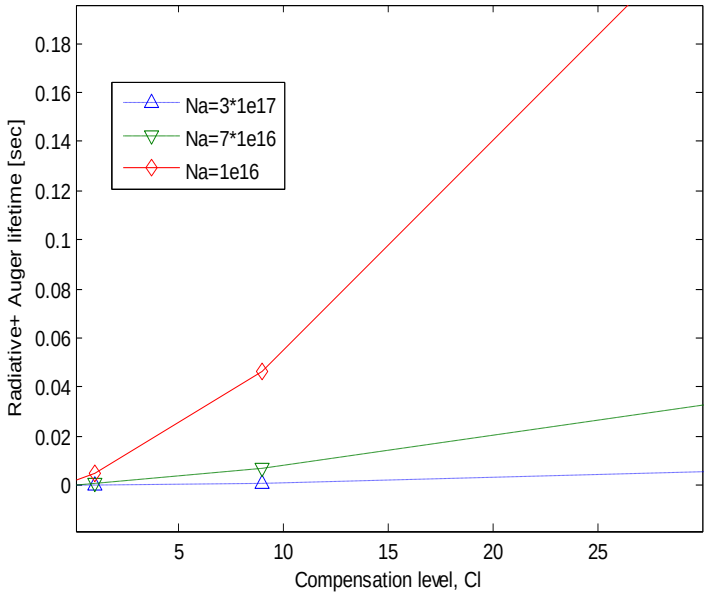

Fig. 6.3: Impact compensation level on intrinsic lifetime of compensated p-Si solar cell.

6.2.2 IMPROVEMENT IN SRH RECOMBINATION LIFETIME

At low injection, standard SRH lifetime equation [7-8] get modified into

$$\tau_{SRH} = \left(N_t \sigma_n \nu_{th}\right)^{-1} \left[\left(\frac{p_0 + p_1}{p_0 + n_0} \right) + \frac{\sigma_n}{\sigma_p} \left(\frac{n_0 + n_1}{p_0 + n_0} \right) \right] \tag{6.4}$$

where N_t is defect concentration, v_{th} is thermal velocity, σ_n ($1-1.4\times10^{-14}$ cm^2) and σ_p ($6-7\times10^{-17}$ cm^2) are electron and hole capture cross section respectively, p_0 and n_0 are equilibrium hole and electron density respectively, p_1 and n_1 are hole and electron concentration calculated at defect energy level.

For p-type compensated silicon, equation 1 can be further reduced as follows

$$\tau_{SRH} = \left(p_0 N_t \sigma_n \nu_{th}\right)^{-1} \left[\left(p_0 + p_1\right) + \frac{\sigma_n}{\sigma_p} n_1 p_0 \right] \tag{6.5}$$

To avoid the trapping effect, N_t is set equal to 10^{12}cm^{-3}. The defect energy levels introduced by iron play vital role in SRH recombination. Interstitial iron [Fe_i] that introduces energy level close to mid-gap is most effective for SRH recombination. For a fixed value of hole concentration, if the donor concentration varies then the hole gets screened out by electron. For this reason, equilibrium hole concentration, p_0 decreases. As a result, SRH lifetime increases as the compensation level increases which is illustrated in fig. 6.4.

The compensation ratio is defined as

$$R_c = \frac{N_A + N_D}{N_A - N_D} \tag{6.6}$$

where N_A and N_D are the acceptor and donor concentration, respectively. The analytical model adopted here in this study has found an increase of 0.2 micro second in SRH lifetime for a factor of 10 changes in compensation ratio which is shown in fig. 6.5.

Fig. 6.4 shows the injection level dependent SRH lifetime for compensated p-Si solar cell. It can be seen that SRH lifetime shifts left for low values of p_0. As compensation is done by adding donor impurity, hole concentration decreases and results in higher SRH lifetime. A linear increase is found in SRH lifetime with compensation level change as shown in fig. 6.5.

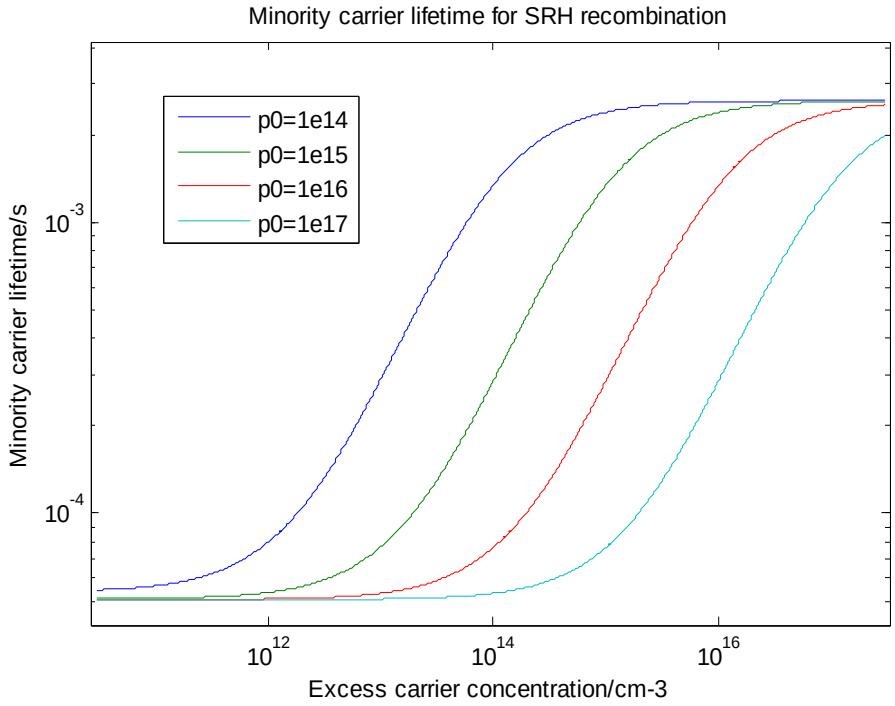

Fig.6.4: Injection dependent SRH lifetime for four different values of p_0 for compensated p-Si solar cell.

Such injection level effects only occur for deep levels impurity, for example Fe_i in silicon, with a much larger capture cross section for minority carriers than for majority carriers. The larger capture cross section for electrons results in a strong injection dependence in p-Si, and causing an increase in lifetime as the degree of compensation is increased.

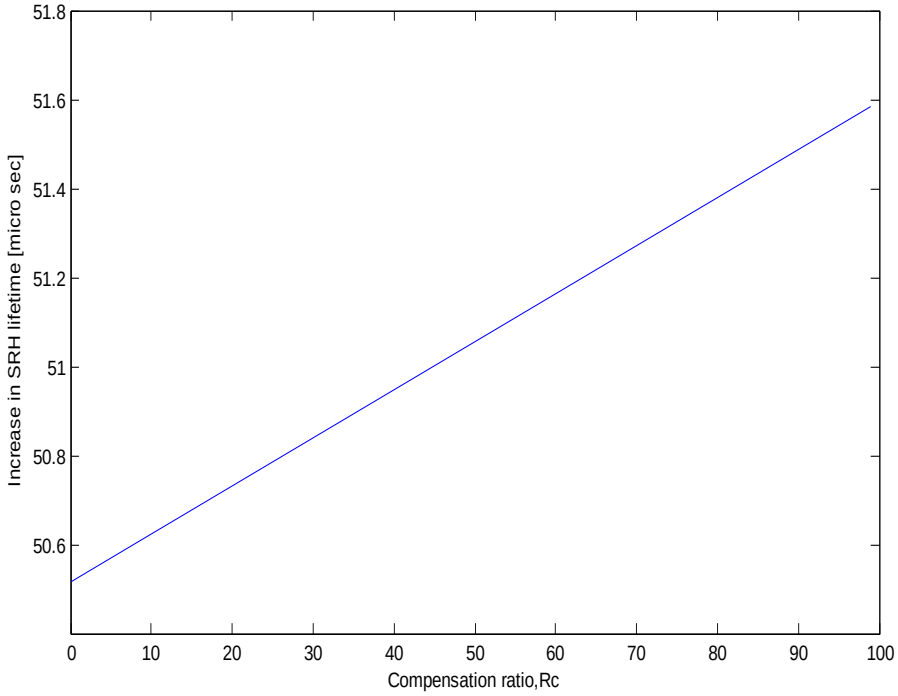

Fig. 6.5: Gain in SRH lifetime due to donor compensation in p-type SoG Si solar cell.

6.2.2 BULK RECOMBINATION LIFETIME

The focus of the research was only to deal with bulk recombination mechanisms associated with SoG silicon. The overall impact of compensation on bulk lifetime can be modeled as

$$\tau_{bulk} = \frac{\tau_{SRH}\tau_i}{\tau_{SRH} + \tau_i} \tag{6.7}$$

here τ_i is the intrinsic carrier lifetime. For deep energy level, SRH recombination lifetime becomes almost equal to minority carrier capture time constant and then dopant concentration has less significance on τ_{SRH}. In this case, $\tau_{bulk} \cong \tau_{SRH}$. It can also be confirmed from the simulated results shown in fig. 6.6.

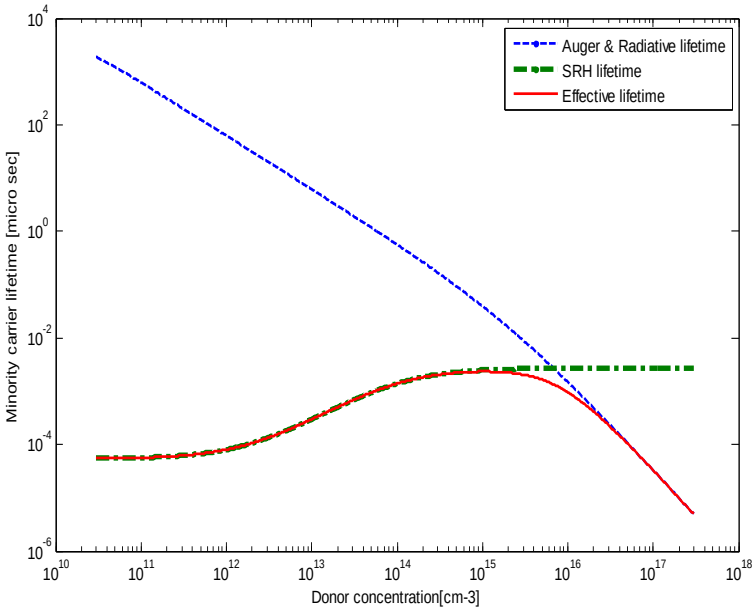

Fig. 6.6: bulk lifetime of minority carrier in compensated SoG silicon.

From fig. 6.6, it is clear that the bulk recombination lifetime is dominated by SRH recombination lifetime for lower compensation, while it follows the same pattern of intrinsic lifetime for donor concentration above 10^{16} cm^{-3}. The maximum of bulk lifetime exists for donor concentration around 10^{15} cm^{-3} for a fixed acceptor concentration of 10^{17} cm^{-3}.

6.3 CONCLUSION

To understand the role of deliberate phosphorus doping in the minority carrier lifetime of iron contaminated boron-phosphorus-compensated p-type solar grade silicon, a numerical study has been performed. This study confirmed that compensation results a significant increase in bulk lifetime of minority carrier. The gain in carrier lifetime is predicted due to the shift in Fermi energy level, carriers screening and reduction in net equilibrium hole concentration. The bulk lifetime of minority carrier reaches its maximum for phosphorus concentration around 10^{15} cm^{-3} if the boron concentrations remain fixed at 10^{17} cm^{-3}.

The utmost importance of this result is the control of compensation level that will facilitate strong improvements in silicon solar cell efficiencies. It could infer that the deliberate

compensation of low-cost SoG silicon will lead to enhance device performance without expensive additional purification steps indeed.

CHAPTER 7

CONCLUSION AND SUGGESTION FOR FUTURE WORKS

7.1 CONCLUSION

This thesis has investigated the limits imposed on the bulk lifetime of crystalline silicon due to intrinsic and extrinsic recombination processes. The injection-level dependence and doping dependence are investigated for both *n*-type and *p*-type silicon of various doping densities, allowing a new general parameterisation for the intrinsic recombination rate in silicon of arbitrary injection level and dopant density to be developed.

Recombination greatly reduce the effective carrier lifetime, therefore, reduces the performance of solar cells, particularly the cell voltage and efficiency. To ensure an accurate interpretation of the recombination lifetime, the impact of principle recombination mechanisms in silicon have been studied analytically using MATLAB. The impacts of Fe contamination in compensated silicon solar cells have performed using the simulation program QSS-MODEL. This program allows the acceptor and donor concentrations to be specified explicitly, enabling the impact of compensation on carrier mobilities to be determined using Klassens‟s model.

7.2 SUGGESTIONS FOR FUTURE WORKS

Based on the results presented here the impacts of others transition metals like Cr, Ni, Ti, Au etc can be investigated. In this thesis, only bulk recombination lifetime due to iron contamination in compensated solar grade has been explored. This thesis has found that compensation leads improved carrier lifetime. Another important recombination called surface recombination can also be explored in SoG silicon. All the results presented here are come from numerical modelling using simulation software. To ascertain the simulated results, a new experiment can be set up. To exploit the bright side of compensation, impurity photovoltaic effect can be investigated in great details. This work can be further extended to study the role of impurity contamination in direct band-gap and multijunction solar cells.

REFERENCES

[1] S. Hegedus and A. Luque, "Status, trends, challenges and the bright future of solar electricity from photovoltaics", Handbook of Photovoltaic Science and Engineering, John Wiley & Sons Ltd., Hoboken, USA (2003).

[2] Helmut Mäckel, "Capturing the spectra of solar cells", PhD thesis, Australian National University, (2004).

[3] S. Rein, "Lifetime Spectroscopy", Springer Verlag, Berlin, Germany (2005).

[4] Schröter W, Seibt M, Gilles D, "High-temperature properties of 3d transition elements in silicon, in electronic structure and properties of semiconductors", ed. By W.Schröter (VHC,Weinheim 1991).

[5] Graff K, "Metal Impurities in Silicon-Device Fabrication", Vol. 24, 2nd ed. (Springer, Berlin, 1999).

[6] Macdonald D, "Recombination and Trapping in Multicrystalline Siliocn Solar Cell", PhD thesis. Australian National University, Australia, 2001.

[7] Hall R., "Electron-hole recombination in germanium", Physics Review 87, 387 (1952).

[8] Shockley W, and Read W, "Statistics of the recombinations of holes and electrons", Physical Rev.87, 835-842 (1952).

[9] Libal J. et al.., "Effect of Compensation and Metallic Impurities on the Electrical Properties of Cz-grown Solar Grade Silicon," Journal of Applied Physics 104, 10450 (2008).

[10] Dubois S. et al., "Effects of the Compensation Level on the Carrier Lifetime of Crystalline Silicon," Journal of Applied Physics 93, 032114 (2008).

[11] Yoon Y, Paudyal B, Kim J, Ok Y, and Kulshreshtha P, "Effect of Nickel Contamination on High Carrier Lifetime n-type Crystalline Silicon " Journal of Applied Physics 111, 033702 (2012).

[12] Gerrad Aissing, "Transition metals in silicon", Phd Thesis, Groningen University, 1988.

[13] S. M. Sze, "Physics of Semiconductor Devices", (John Wiley & Sons, New York, 1981).

[14] F. D. Auret, R. Kleinhenz, C. P. Schneider, "Deep level transient spectroscopy of defects introduced by resistive evaporation of metals on silicon", Appl. Phys. Lett. 44, 209 (1984).

[15] E. Ohta, K. Kakishita, H. Y. Lee, "Introduction of defect levels in resistive evaporated n-Si Schottky barrier diodes" ,J. Appl. Phys. 65, 3928 (1989).

[16] O. Kumagai, K. Kamko, "Fe ion dose dependence of deep levels in Si P^+ - n Junction", J. Appl. Phys. 51, 5430 (1980).

[17] O.V. Aleksandrov, V. V. Koslovskii, V. V. Popov, B. E. Samorukov, "Diffusion of impurities from implanted silicon layers by rapid thermal annealing", Phys. Status Solidi (a) 110, K61 (1988).

[18] F. Beeler, O. K. Andersen, M. Scheffler, "Theoretical evidence for low-spin ground states of early interstitial and late substitutional 3d transition metal ions in silicon", Phys. Rev. Let. 55, 1498 (1985).

[19] H. Feichtinger et al. 13^{th} International conference on defects in semiconductors, p.855, Coronado, 1984.

[20] A Chantre, L.C. Kimmerling, 14^{th} International conference on defects in semiconductors, p. 387, Switzerland, 1986.

[21] A Chantre, D. Bois, "Metastable defect behavior in silicon: charge-state-controlled orientation of iron-aluminum pairs", Phys. Rev. B 31, 7979 (1985).

[22] Ref. in K. Graff, "Current understanding of the behavior of transition metal impurities in silicon", Semiconductor silicon, p. 751, NJ, 1986.

[23] S. D. Brotherton, P. Bradley, A. Gill, "Electrical observation of Au-Fe complexes in silicon", J. Appl. Phys. 55, 952, (1984).

[24] H. Lemke, "Eigenschaften einiger Störstellenkomplexe von Zink in Silizum", Phys. Status Solidi (a) 72, 177 (1982).

[25] G. Zoth, W. Bergholz, Extended abstracts Fall meeting, p. 643 (Electrochemical Soc. Phoenix, Arizona), 1991.

[26] W. Bergholz, G. Zoth, H. Wendt, S. Sauter, G. Asam, Siemens Forsch.- u. Entwickl.-Ber. 16, 241 (1987).

[27] K. Graff, H. Pieper, "The properties of iron in silicon",J. Electrochem. Soc. 128, 669 (1981).

[28] L. C Kimmerling, "Defect characterization by junction spectroscopy", Defects in semiconductor, Elsevier, p. 85,(1981).

[29] H. Lemke, "Energieniveaus und Bindungsenergien von Ionenpaaren in Silizium", Phys. Status Solidi (a) 76, 233 (1983).

[30] J. Schön, H. Habenicht, M. C. Schubert, and W. Warta, "Simulation of iron distribution after crystallization of mc silicon", Solid State Phenomena **156-158,** 223-228 (2009).

[31] D. Macdonald, J. Tan, and T. Trupke, "Imaging interstitial iron concentration in boron-doped crystalline silicon using photoluminescence",Journal of Applied Physics **103,** 073710-1 to 073710-7 (2008).

[32] T. U. NærLand, L. Arnberg, and A. Holt, "Origin of the low carrier lifetime edge zone in multicrystalline PV silicon", Prog. Photovolt: Res. Appl. 17, 289-296 (2009).

[33] D. Macdonald, A. Cuevas, A. Kinomura, Y. Nakano, and L. J. Geerligs, "Transition-metals profile in multicrystalline silicon ingot" , Journal of Applied Physics **97,** 033523-033527 (2005).

[34] M. Rossberg, M. Naumann, K. Irmscher, U. Juda, A. Lüdge, M. Ghosh and A. Müller, "Investigation of defects in the edge regions of multicrystalline solar silicon ingots", Solid State Phenomena 108 -109, 531- 536 (2005).

[35] M. Rinio, C. Ballif, T. Buonassisi, and D. Borchert, "Defects in deteriorated border layer of block-cast multicrystalline silicon ingots", In 19th EUPVSEC, Paris (2004).

[36] A.A. Istratov, H. Hieslmair, and E. R. Weber, "Iron and its complexes in silicon", Appl. Phys A: Material Science and Processing 69, 13 – 44 (1999).

[37] J. Nelson, "The physics of solar cells", Imperial college press, London (2003).

[38] Mauro Zanuccoli, "Advanced numerical simulations of silicon-based solar cells", PhD thesis, University of Bologna, Italy (2012).

[39] J. Dziewior, W. Schimd, "Auger coefficients for highly doped and highly excited silicon", Appl. Phys. Lett. 31 (5) 346-8, (1997).

[40] A. Hangleter, R. Hacker, "Enhancement of band-to-band Auger recombination by electron-hole concentration", Phys. Rev. Lett. 65 (2), 215-18, (1990).

[41] P. P. Altermatt, J. Schmidt, G. Heiser, and A. G. Aberle, "Assessment and parameterization of Coulomb-Enhanced Auger recombination coefficients in lowly injected crystalline silicon", J. Appl. Phys. 82 (10), 4938 -44 (1997).

[42] S. W. Glunz, D. Biro, S. Rein, and W. Warta, "Field-effect passivation of the SiO2-Si interface", J. Appl. Phys. 86 (1), 683 -91 (1999).

[43] A. G. Aberle, "Crystalline silicon solar cells – Advanced surface passivation and analysis", (University of New South Wales, Sydney, 1999).

[44] A. Cuevas, D. Macdonald, "Measuring and interpreting lifetime of silicon wafers", Solar Energy 76 (2004) 255-262.

[45] R.A. Sinton and A. Cuevas, "A quasi-steady-state open- circuit voltage method for solar cell characterization", 16th European Photovoltaic Solar Energy Conference, 1–5 May, Glasgow, UK, 1152–1155 (2000).

[46] V. Grivickas, D. Noreika, J.A. Tellefsen, "Surface and Auger recombination in silicon wafers of high carrier density", Lithunian Physics Journal 29 (5), 48-53, (1989).

[47] W. Zulehner, "Growth conditions of the metal-contaminated Cz-Si crystals", (2000).

[48] M.A. Green, "Solar cells- operating principles, technology and system applications", (Prentice-Hall, 1986).

[49] J. Libal et al.., "Effect of Compensation and Metallic Impurities on the Electrical Properties of Cz-grown Solar Grade Silicon," Journal of Applied Physics 104, 10450 (2008).

[50] S. Dubois et al., "Effects of the Compensation Level on the Carrier Lifetime of Crystalline Silicon," Journal of Applied Physics 93, 032114 (2008).

[51] F.E. Rougieux, D. Macdonald, and A. Cuevas, "Transport properties of p-type compensated silicon at room temperature", Prog. Photovolt: Res. Appl. (2010).

[52] F.E. Rougieux, M. Forster, D. Macdonald, A. Cuevas, B. Lim, and J. Schmidt, "Recombination activity and impact of boron-oxygen releated defect in compensated n-type silicon", IEEE Journal of Photovoltaics **1**, 54 (2011).

[53] D. Leblanc, and K. PutyeraP, "New resistivity/dopant density model for compensated Si", Trans.Nonferrous Met. Soc. China **21**, 1172 (2011).

[54] D. Macdonald and A. Cuevas, "Recombination in compensated crystalline silicon for solar cells", Journal of Appl. Phys. **109**, 043704 (2011).

[55] J. Veirman, S. Dubois, N. Enjalbert, J.P. Garandet, and M. Lemiti, "Electronic properties of highly doped and compensated solar-grade silicon wafers and solar cells", Journal of Appl. Phys. **109**, 103711 (2011).